Use of the Zebrafish to Explore the Connection of Pituitary Development with Congenital Craniofacial Syndromes

Use of the Zebrafish to Explore the Connection of Pituitary Development with Congenital Craniofacial Syndromes

Lisa Tsay

A Thesis in the Field of Biology

for the Degree of Master of Liberal Arts in Extension Studies

Harvard University

May 2024

Abstract

This thesis project is focused on analyzing pituitary development using the zebrafish study model. Our lab focuses on studying craniofacial malformations using complementary models that include human and other mammalian cells, mouse and zebrafish. Investigation in the Esrp1/2 mouse model revealed affected pituitary development. Esrp1/2 are known genetic causes of craniofacial developmental issues such as cleft lip palate. Visualization of pituitary development may aid in future research implicating *ESRP1* and *ESRP2* as being causative of growth hormone deficiency diseases such as congenital hypopituitarism. The effect of *esrp1* and *esrp2* in zebrafish on both midfacial morphogenesis and its effect on multiple germ layers have implications around there being multiple germ layer origins of the pituitary which is a currently debated topic in the field of embryology and whether the same pathways in zebrafish are evolutionarily conserved in enough ways to serve as a model for this possible research. We hypothesized that it is possible to visualize the development of the pituitary that models what is currently known about pituitary development in zebrafish.

Using a number of methodologies such as whole-mount *in situ* hybridization (WISH), multiplexed *in situ* hybridization (RNAscope), and time-lapsed imaging under fluorescent imaging microscopes and light sheet microscope, we were able to visualize the pituitary at various stages of development reflecting what is currently theorized around how the pituitary develops. Additionally, we present efforts around the creation of a LIM homeobox protein (*lhx3)* transgenic reporter line which could be used for future

research implicating mutations in *ESRP1*/*2* as being causative for both cleft lip palate disorders and congenital hypopituitarism. As the author of this thesis paper, Lisa Tsay carried out all the experiments outlined and presented in the methods, results, and discussion sections under the guidance of Drs. Eric Liao and Shannon Carroll.

Dedication

I dedicate this thesis to the memory of my father. He pursued upper education with the hopes of building a better life for his family. I wish to emulate his pursuit and hope that my efforts to complete this thesis further show how much he has succeeded in bringing hope and prosperity to our entire family.

Acknowledgments

First, I would like to thank my friends and family. This includes my mom, all five of my siblings, my uncle David, Robert Hill, Marc Osbourne, Laura Spencer, Steven Powell, Jonathan Spencer, George James, and countless others whose names would not fit on a single page. Without your support every day, I would not have the fortitude to take on this work.

I would also like to thank my former coworkers at Massachusetts General Hospital. Collectively, you believed in me, inspired me, gave me guidance on my career life, and taught me so much about research. A few names among them include Dr. Sara Pai, Dr. William Faquin, Dr. Peter Sadow, Dr. Juhyun Oh, Dr. Jennifer Kim, Cheryl Greene, Natalia Queenan, Casey Tsimbal, Kim Northrup, and Jacqueline Nolan.

Next, I would like to thank Dr. Shannon Carroll. Shannon was the one who inspired me to focus my thesis project on this topic and taught me the essentials of performing this research. She is not only someone I consider a friend but also a mentor and a role model.

Finally, I would like to thank Dr. Eric Liao. Without his support, this entire thesis project would not be possible. I am truly proud of all the things we have accomplished together these past few years and eternally grateful I was able to meet you. Thank you from the bottom of my heart.

Table of Contents

List of Tables

List of Figures

Chapter I

Introduction

Congenital hypopituitarism (CH) is a disease resulting from deficiencies in pituitary hormones, affecting 1 in 4000 to 1 in 10000 live births (Bosch et al., 2021). CH is a disease resulting from genetic mutations affecting the development of the pituitary or damage caused to the developing pituitary. Presentation of CH can include a wide variety of symptoms such as stunted growth, hypoglycemia, thyroid dysfunction, and septo-optic dysplasia resulting from deficiencies in key pituitary hormones (Cullingford et al 2023). Several genes tied to families have been associated with CH but over 80% of those cases do not have a known genetic cause (Vishnopolska et al., 2021). From this, we can predict additional genes as well as gene-gene and gene-environment interactions contribute to congenital hypopituitarism.

In this thesis, we use the terms pituitary and adenohypophysis interchangeably. The adenohypophysis refers to the anterior lobe of the pituitary which makes up most of its overall tissue (Adenohypophysis). This tissue is thought to derive from the adenohypophysis cranial placode (Ueharu et al., 2017) which is theorized to form from the merging of two distinct bilateral tissue primordium early in development (Herzog 2004). While the elaborate cellular changes that occur during the development of cranial placodes have been well described in mammals (Singh et al., 2016), there is still debate about whether the specifics of early zebrafish pituitary development closely mirror mammalian pituitary development enough to be used as a possible model for studying CH and other early pituitary developmental disorders. The known differences in pituitary

development that occur following the posterior migration of the merged adenohypophyseal placode in zebrafish as compared to other mammals are why we describe these tissues and associated genes as being orthologous as opposed to analogous. A closer examination of the similarities in early development of the pituitary between both zebrafish and mammalian study models could justify using the zebrafish as an additional model for pituitary developmental disorders.

Mammalian models, particularly mice and rats, are widely favored research animal models but there are difficulties using these models for in vivo development studies. These considerations include small litter sizes, the typical sacrifice of a pregnant female to observe changes in developing mouse pups, and the inability to track multiple developmental time points within the same mouse pup. In comparison to mammalian models, zebrafish have large clutch sizes with external development, are highly amenable to genetic modifications, and have transparent embryos that could be utilized for live imaging through development without sacrifice of the embryo. By utilizing the translucence of zebrafish embryos, modern imaging modalities such as light sheet microscopy could be used if it were possible to create a transgenic fish line tied to genes directly associated with the developing pituitary.

Our lab studies the genetic regulation of craniofacial development using zebrafish, mouse, and human cell models. Esrp1, and its paralog Esrp2, are epithelial-specific regulators of mRNA alternative splicing, which refers to when a single gene may code for multiple mRNA transcripts and gene products (alternative splicing). Esrp1/2 were found to be required during craniofacial development in mice and zebrafish (Carroll et al., 2020, Bebee et al., 2015) and ESRP1/2 gene variants are associated with human

orofacial clefts (Cox et al., 2018, Leslie et al., 2013). We discovered evidence of disrupted pituitary development in Esrp1/2 knockout mice and zebrafish (Figure 1). This evidence along with recent studies challenging the currently accepted theories around what tissue primordium certain placodal tissue originates from is of interest to our lab's current studies.

Given that there is a likely connection between functions of ersp1/2 and the convergence of the face in relation to the development of the pituitary, we believe this connection merits further investigation into the development of the adenohypophysis of the zebrafish within both wildtype and mutant esrp1/2 fish.

Definition of terms

Adenohypophysis: The term used in place of “pituitary” to describe the orthologous organ of mice and zebrafish, which is the major gland of the endocrine system that controls other parts of it. It is located at the base of the brain. Both pituitary and adenohypophysis are used interchangeably in the literature when discussing related endocrine activity.

Childhood Onset Combined Pituitary Hormone Deficiency (CPHD): a childhood condition where the pituitary is unable to produce sufficient growth hormones. It is not well understood and upward of 30 or more genes are thought to contribute to the condition.

Early Puberty: Described as a stage of development occurring within the first six months of humans’ lives and is not well understood. It is believed that this stage of infancy acts as a time of hormonal priming for sex-specific gamete generation.

Ectoderm: One of the three embryonic germ layers that is associated with the formation of the neural tube and develops into the central nervous system, skin, exocrine glands, and the anterior pituitary.

Endoderm: One of the three embryonic germ layers that are associated with the development of the digestive tubes, respiratory tubes, pharynx, and other accessory organs related to digestion and the endocrine system.

Hypopituitarism: Refers to the broad state of having a deficiency in pituitary-associated hormones. The state is described by several notable symptoms including facial cleft, severely stunted growth, etc.

iPSCs: An acronym for induced Pluripotent Stem Cells. We discuss iPSCs briefly to address the inadequacies and difficulties faced when using this study model to understand early pituitary developmental disorders.

esrp1, esrp2: *esrp1/2* are paralogs and are regulatory proteins associated with epithelial differentiation and formation of the palate. *esrp2* is associated with orofacial clefting in humans. When decreased expression of *esrp1/2* cannot be compensated for orofacial abnormalities including clefts arise. (Carroll et al., 2020).

lhx3: A gene highly associated with the pituitary and related pituitary disorders. *lhx3* is highly expressed within the anterior pituitary of zebrafish, and more specifically Rathke's Pouch. *lhx3* is also expressed in the hindbrain, the spinal cord, and motor neurons at later points of development.

Midface, Frontonasal Ectodermal Zone (FEZ), Midline morphogenesis: When the structure of the face is considered three different areas, the midface is defined as the middle section including the nose, associated bony structures and portions of the upper lip and jaw. Within the developing midface is an area known as FEZ, an area of high

complexity where multiple germ layers form different structures of the face and may be more prone to developmental structural defects, such as cleft palate. Midline morphogenesis is the process during early development in which the tissues from each side of the head grow toward each other and morph together to form the different structures of the face.

Neural Crest Cells (NCCs): refer to cells in early development across species that migrate and differentiate into several cell types within the neurocranium of the respective species.

Optical Tomography: This usually refers to a computed reconstruction of the inside of an object. In the context of this project, we will be attempting optical tomography utilizing a transparent in-vivo study model with fluorophore-tagged proteins of interest. Construction of a 3D model will be done via a light sheet fluorescent microscope and up to a 72-hour scanning period.

Orofacial cleft: Orofacial cleft is a term used to describe the physical abnormalities involving a developmental failure of the upper lip and palate to fuse.

Ortholog, orthology, orthologous: Terms that refer to genes that became differentiated due to speciation events, but which have conserved functions within each of the compared species.

pitx3: A gene for a transcription factor in humans that is associated with the differentiation of neurons. The gene within zebrafish highly localizes around the pituitary and surrounding midfacial neurocranium.

Placode: a term used to describe a thickening of the endoderm or ectoderm. Here, the placode is used to refer to the preliminary structures that eventually merge and move posteriorly to eventually form the mature pituitary organ.

Single Cell RNA Sequencing (RNA Seq), lineage tracing: a genomics technique allowing for analysis of the transcription of mRNA and can allow researchers to compare differences in transcription of target mRNA from one cell to another. This is both used to identify rare/small cell populations and for lineage tracing of cells which allows tracking of individual cells and the cell fates over generations of cells.

Transgenesis: Refers to the introduction of foreign DNA into the germline of a different species. In this case, we use transgenesis to refer to our generation of transgenic zebrafish reporter lines.

Whole-Mount In-Situ Hybridization (WISH): A 3-day in-situ hybridization technique to determine where within zebrafish embryos mRNA from a target gene is expressed.

Background of the Problem

The pituitary is responsible for numerous functions in the human body such as growth, metabolism, and reproduction throughout our lives. The pituitary has two main lobes which produce many of the body's essential hormones. The posterior pituitary produces antidiuretic hormone (vasopressin/ADH) and oxytocin. The anterior pituitary produces human growth hormone (HGH), thyroid-stimulating hormone (TSH), luteinizing hormone (LH), follicle-stimulating hormone (FSH), prolactin, and adrenocorticotropic hormone (ACTH) (Pituitary Gland, 2022). The pituitary is located at the base of the brain, directly below the hypothalamus. The hypothalamus is a gland that coordinates homeostasis based on feedback from both the endocrine and the nervous systems (Hypothalamus, 2022.). The two organs are connected by the infundibulum which is a stalk of nerves and blood vessels. The hypothalamus maintains homeostasis using the hormones it produces to influence the hormone activity of the pituitary gland. (Hypothalamus, 2022).

Disorders of the pituitary occur when the amount of produced hormone deviates from the normal range. Because pituitary disorders occur very slowly, they sometimes present with symptoms like other diseases or are not diagnosable until the signs of the disorder have already become problematic. This is especially true in the case of early development where deficiencies in pituitary activity have long-lasting effects that affect them over their entire lifespan. A developmental stage of infancy known as "mini puberty" occurs in both males and females within the first six months of life and is not well understood (Hietamaki et al., 2022). Most of what has been studied for topics such as mini puberty has been researched through reporting of rare medical cases involving

affected newborns, young children, and genetic analyses of the affected and their families. The term for the broad deficiency of pituitary hormones is known as hypopituitarism and the associated condition is 'Childhood Onset Combined Pituitary Hormone Deficiency (CPHD)'. Currently, there is still no consensus on what causes hypopituitarism (Gregory & Dattani, 2020; Hietamaki et al., 2022).

Rodent models have been pivotal in the understanding of the genetic regulation of pituitary development but are not an optimal model to use when tracking the development of the pituitary in utero. Studying developmental changes across time is labor and resource-intensive as it requires the sacrifice of the animal. The long-term effects of pituitary deficiencies would ideally be studied in the same organism or genotypic cohort over time. While mice breed frequently, litters of inbred mice are typically 4-8 individuals, limiting the experimental sample size when larger numbers of offspring may be needed to find compound recessive phenotypes.

In vitro protocols have been used to study pituitary development, particularly with the specification and differentiation of the hormone-producing cells (Zimmer et al. 2016). The use of induced pluripotent stem cell (iPSC) in vitro models, while being able to model aspects of the pituitary outside of the body, cannot completely replicate the function of the pituitary within a naturally functioning environment or display its effects on organ systems outside of the pituitary's immediate vicinity or overtime (Doss & Sachinidis, 2019). *In vitro* models also require expensive and time-consuming upkeep to maintain the differentiation of the desired cell types (Saha & Jaenisch, 2009). Some essential materials such as Matrigel undergo supply shortages which can jeopardize experiments (Knoepfler et all, 2022). Substitute materials exist but labs may be pressured

to repeat experiments with trusted materials to verify their results for acceptance in the scientific community (Walker et al., 2019).

In addition to considerations around the choice of study model, there are microscopy-related considerations. Older models of microscopes cannot give us precise enough information on how known related proteins migrate, are over or under-expressed, or otherwise malfunction in existing animal models (Prakash et al., 2022). Preparation of sample slides can be laborious and involve multiple protocols before analysis, such as staining or clearing of samples for optical clarity (Ariel, 2017). This also does not circumvent the problem of a need to model pituitary development or malfunction in a live organism over time. This can be compared to seeing a single photograph when what would be desired is to capture a full-length movie in high definition.

Zebrafish is an excellent model to study pituitary development and disorders and have become more popular in general as a study model for disease modeling for other organ systems such as the heart, lungs, and craniofacial disorders. Zebrafish can produce hundreds of fertilized embryos per mating, develop quickly, are more amenable to genetic modifications, and are transparent in their early development, making them an attractive model to use for early developmental *in vivo* studies (Teame et al., 2019). Even though previous studies have been published detailing zebrafish pituitary development, many details remain on pituitary primordium origins, cellular mechanisms, and genetic regulation. Protocols involving the embedding of zebrafish embryos in agarose for live imaging with light sheet microscopes could allow for the imaging of embryos for up to 72 hours without detriment to the zebrafish's development (Weber 2014, Kaufmann et al., 2012).

Discussing the usage of zebrafish to study pituitary development means examining what we currently know about pituitary development in mice and humans and examining further whether the zebrafish adenohypophysis shares enough of a conserved developmental pathway early on in pituitary development. The origins of sensory placodes are still debated and are thought to develop from a common preplacode primordium layer, likely the anterior neuronal ridge (Schlosser 2005, Koontz 2022, Sheng 1997). In the case of the adenohypophysis, two distinct placodes merge to form a single pituitary placode around 28 hpf (Herzog et al, 2003). The pituitary placode, in conjunction with simultaneous axis extension in development, then migrates posteriorly until about 72 hpf, where the pituitary has been described as morphologically distinct at this point (Chapman 2005). In mammals, pituitary development continues as the placodal cells begin to invaginate and eventually bud off from the ectodermal layer in the formation of what becomes Rathke's pouch. The newly formed pouch then migrates upward until it wraps around and merges with the base of the hypothalamic stem and matures into the fully formed pituitary (Suga et al. 2016). When compared to mammalian development, it has been found in developing zebrafish that no invagination analogous to the formation of Rathke's pouch occurs. Instead, a reorganization of the placodal cells from a medial location to posterior locations and lateral cells of the placode to anterior occurs as the pituitary placode matures (Herzog et al. 2003). Following that, the pituitary settles in its final location as axis extension continues with similarities in the extension of the notochord but major differences in each animal's specific development, such as with the formation of the cervical spine in humans as opposed to the straightening and lengthening needed for proper body formation in the zebrafish (Developmental

Mechanism).Several mouse pituitary transcription factors are much less prevalent in zebrafish, requiring careful selection of the gene targets of choice for pituitary studies. *Lhx3*, which is required for pituitary cell lineage determination (Sheng et al 1996) is one such gene that is present throughout the development of the pituitary in both mice and zebrafish. *Pitx3* has been found to be needed for cell proliferation, survival, and differentiation based on its concentration and is associated with craniofacial disorders such as Rieger's syndrome involving defects in the formation of the eye chambers, intellectual disabilities, and growth hormone deficiency (Zhu et al 2005). *pomca*, which is shown to have connections to metabolism and reproduction, is expressed early in development (~20 hpf) within the pituitary, hypothalamus, and various other structures related to the nervous system (Toda 2017).

Other research involving the study of the pituitary/adenohypophysis in zebrafish is limited. One paper involves the understanding of *bmp*, *fgf*, and *shh*s' roles within the pituitary (Liu et al., 2008). Other papers discuss *shh* and how differentiating cell fates are determined for endocrine cells during pituitary development (Guner et al., 2008; Herzog et al., 2003; Liu et al., 2008). Another related to pituitary development studied *eya1* and its role in pituitary development (Nica et al., 2006). Among more recent zebrafish pituitary literature is an investigation into the germ layer origin of the different cells of the pituitary (Fabian et al., 2020). Unlike what has been previously believed, the authors were able to find contributions to the cells of the fully formed pituitary from the endoderm, as opposed to those cells exclusively originating from the ectoderm as previously thought. The results of this paper bring questions of cell migration and midline

morphogenesis and help us ask additional questions for this project that help quantify what we may learn.

A topic that has been of major importance to our lab is the investigation of the role of *Ersp1* and *Esrp2* in regulating midface morphogenesis and orofacial clefts. *Esrp1 and Esrp2* are paralogs and are regulatory proteins associated with epithelial differentiation and formation of the palate (Warzecha et al., 2009). ESRP2 is associated with orofacial clefts in humans (REF). Misalignment of the processes regulated by these genes or deficiencies in one or a combination of those genes results in varying severities of midfacial defects including orofacial clefts (Carroll et al., 2020, Lee et al., 2020) that have been extensively described in our lab's past research and continues to be a major focal point of our continuing research.

While investigating the role of *Esrp1* and *Esrp2* in orofacial development, our lab observed defects in pituitary development within *Esrp1/2* knockout mice. Figure 1 shows mouse specimens with a series of stained tissue sections for each one (B-E, 1-5 for each specimen). Figures 1B and 1C represent wild-type mice and figures 1D and 1E represent *Esrp1/2* knockout mice. The major anatomical difference we observed involved a failure of the anterior pituitary to develop normally. This is relevant because CPHD is associated with deficiencies of the anterior pituitary from which many of these hormones are produced (Fang et al., 2016). Congenital hypopituitarism is also associated with abnormalities within the anterior pituitary, specifically Rathke's pouch (Gregory & Dattani, 2020).

Question and Hypothesis

Given that current theories around the origins of the pituitary continue to be debated, the question is whether it is possible to lend further evidence to the existing theories around the development of the adenohypophysis in the zebrafish and whether mechanisms known to be conserved within mice and humans are evolutionarily conserved in the zebrafish model. We hypothesize that many of the mechanisms regulating the development of the adenohypophysis in zebrafish are evolutionarily conserved in mice and humans based on our findings outlined in Figure 1 in a mouse model along with what is known about *esrp1/2*'s role within zebrafish craniofacial development.

With this central question and hypothesis in mind, the purpose of this thesis project will be to analyze normal and affected pituitary development by utilizing both normal and *esrp1/2* mutant zebrafish models to compare the expression of key pituitary-related genes which included lhx3, pomca, and pitx3. We used staining protocols such as whole mount in situ hybridization and RNAscope to compare wildtype and *esrp1*, *esrp2* knockout mutants. In terms of novel methodology, we used light-sheet microscopy to visualize pituitary development in real-time using an incross of transgenic fishlines to facilitate imaging and describe the ability of the techniques to visualize the development of the pituitary placodes. Additionally, we describe our attempts to create a transgenic fish line using CRISPR guides designed for *lhx3*. This research will bolster our understanding of normal pituitary development and the role of the epithelial tissue in relation to pituitary development when known regulators of epithelium are disrupted.

Additionally, it will further validate the zebrafish as a model of pituitary developmental disorders, which includes identifying causative factors of CH.

Chapter II.

Methods and Materials

The following section describes the breadth of experimental methods used to generate the data contained within this project. They include a variety of zebrafish husbandry techniques, novel imaging techniques, microbiology, histology, and genetics protocols that have been tailored for the use of the zebrafish study model.

Fin Clipping

The regenerative properties of the zebrafish allow for tissue samples to be collected from the tail fin to obtain genetic material for analysis. Zebrafish are raised to approximately 3 months of age or to a substantial size before carrying out the procedure. A solution of 240 mL of aquatic system water and 10 mL of Tricaine are set in the breeding tank to anesthetize the fish and fish are placed into the breeding tank with solution until properly sedated. Proper sedation is achieved at the point where the fish ceases to struggle while undergoing the procedure without its gills ceasing to move or 10 minutes, whichever comes first.

Once sedated, using a pair of tweezers and a cutting instrument such as a razor blade or scalpel, a section of the tail fin is cut off and placed into a microtube and labeled for identification. Removal of more than 30% or more of the tail fin is detrimental to the fish’s health and care should be taken to take a minimal amount needed for experiments.

Genotyping and PCR

Following collection of clipped fins or other tissue specimens, tissue is placed in 100 µL of 50 mM Sodium hydroxide and undergoes a digestion program at 95°C in a standard thermocycler (Eppendorf) for 30 minutes. The digestion process is then stopped by the addition of 1/3 volume 1M Tris HCL (33 µL). Our standard PCR protocol calls for the use of Taq Polymerase (Promega M7833), H20, forward primer, reverse primer, and the DNA sample in a standardized ratio (10:7:1:1:1 respectively) uniformly across all PCR samples. Most genotyping done for this project involved the amplification of tdTomato gene products, which have an optimized annealing temperature of 54°C. These PCR products were then either run on an agarose gel, sent to CHOP Genomics Core for fragment analysis, or sent to Azenta Inc. for detailed Sanger sequencing results.

Breeding, Embryo Collection and Monitoring Development

For any planned mating, adult fish of both sexes are segregated into small breeding tanks in the afternoon prior to the morning of the planned mating. Females are identified by having a larger belly indicating the carrying of eggs and males are identified as having narrow arrow-like bodies.

In the morning, usually between 8 am and before noon, the dividers for breeding tanks are removed and the fish are allowed to mate. The tanks are monitored in short intervals to ensure precise timing of embryo collection. Mating pairs may produce more embryos when the tanks are tilted, and the water level is lowered to keep fish in closer proximity during the breeding process. Fish are separated from each other and placed back in their receptive tanks either when an adequate number of eggs are laid or whenever the user decides to discontinue monitoring of the breeding pairs.

The collection of eggs should occur shortly after the eggs are laid. After the removal of the breeding pairs, the egg-containing system water is collected through a net. Eggs are gently rinsed in additional system water to remove debris and then placed in a 20 mm petri dish with sufficient embryo medium at a stocking density of 50 embryos per plate or less. Embryo plates are then stored in an incubator at a constant temperature of 28°C.

Embryo plates are cleaned and monitored daily to ensure normal development until 5-6 days of age before being placed onto the fry rack of the aquarium. Beyond this initial growth stage, care for the embryos through their early development is provided by the Zebrafish core and generally follows guidelines set by IACUC, "The Zebrafish Guidebook", CHOP's Zebrafish core, and ZIRC.

Gel Electrophoresis and Imaging

All standard gel analysis was run on 1.5% agarose gels using basic agarose powder, 1x TAE buffer, and 8 µL of ethidium bromide in liquid form added after melting of agarose, letting it slightly cool, gently incorporating it into the liquid mixture and pouring the mixture into the gel molds. Each gel is run at the standard settings of 100 volts for 1 hour with a maximum amp range of 500 amperes. Each gel was run with a 50-base pair ladder and both positive and negative controls where possible. In the example of genotyping fish for tdTomato this included running PCR samples alongside the plasmid of tdTomato, a positive tdTomato screened fish DNA sample, and a negative wildtype control. All gel images contained in this paper were imaged using an Axygen Gel documentation system and were imaged under a 302 nm wavelength lightbulb with varying exposure depending on the intensity of the samples.

CRISPR/Cas9 Preparation

Gene-specific crRNA oligonucleotide guides are designed and purchased through a company such as IDT. These guides, along with a green fluorescent protein (gfp) crRNA guide are reconstituted to a 100 nM concentration. Each guide (gene of choice and gfp) is mixed with tracrRNA and buffer/nuclease-free water in a ratio of 1:1:2 respectively. Each mixture is then incubated at 95°C for 5 minutes and then allowed to cool to room temperature. Continuing to keep each mixture separate, an RNP complex is assembled by mixing the gene-specific mixture, diluted Cas9 enzyme (IDT Catalog 108105 ,1 µL diluted in 4 µL nuclease-free water) and working buffer in a ratio of 2:1:1 respectively. Both mixtures are incubated at 37°C for 10 minutes and allowed to cool to room temperature. To use for injection, each solution is mixed in equal parts along with a plasmid such as tdTomato and phenol red (Sigma Aldrich P0290) which is used as an injection indicator.

Zebrafish Embryo Microinjections

Preparation for injections begins the day before by setting up mating pairs the night before and preparing 3% agarose injection mold plates. In the morning, the breeding pairs are allowed to mate, and glass capillary needles are cut to create a bevel and calibrated to inject approximately 2 nL per injection pump. Once eggs have been laid, the eggs are collected promptly, screened for health quality, and then dry loaded into a room temperature injection mold, followed by adding enough liquid in the plate wells to prevent drying out of the embryos.

Either by using an injector apparatus or by freely holding the glass needle holder, each embryo is injected with the prepared fluid. Injections are most effective when

injected either directly into the cell or into the interstitial space between the yolk and the embryo. Injection of embryos must take place within the first 30 minutes following the formation of embryos to ensure injection of the prepared fluid happens during the 1-cell stage of the embryos' development. Failure to do so reduces injection effectiveness and could otherwise result in chimeric expression of the target gene within the developing fish. Once all embryos have been injected, they are placed in a labeled petri dish with sufficient embryo medium and monitored at frequent intervals to ensure the health of the injected embryo clutch.

Morpholino Titration and Calculations

Morpholinos refer to oligomer molecules that are used to restrict access to small segments of DNA, making them useful for gene knockdown experiments (Moulton 2017). Our lab used morpholinos to ensure higher consistent numbers of embryos with a demonstrated phenotype among a clutch of embryos with a known genotype, which helped our lab avoid genotyping labor. Titration of the concentration of the morpholino was done both to ensure what concentration would be needed for the effectiveness of the morpholino and to test for toxicity among different clutches of injected embryos. Table 1 depicts the calculations used to calculate the different concentrations of morpholinos used and our evaluation of the effectiveness of the morpholino for each of our injection test groups. Additionally, control morpholino injections (Gene Tools Random Control 25N) were done for *esrp1* knockout mutants to ensure our mutant phenotype was a result of the *esrp2* morpholino's mechanism and not a result of potential injection injuries to the early embryos.

Verification of Transgenesis

24 hours following the injection of a Cas9 construct, embryos were subjected to a prolonged heat shock protocol set at 38°C for a span of no longer than 2 hours. After exposure to the higher temperature, the embryos are then placed back into a normal incubation temperature of about 28°C for at least an hour to allow the heat shock signal to intensify. Embryos are then screened for high-intensity expression and widespread expression of the fluorophore. Screening embryos with these criteria indicates a higher likelihood that the Cas9 construct was able to be inserted into the germline of the specimen. The fluorophore expression induced by the heat shock protocol can be observed for several days afterward.

Embryos exhibiting both a high spread of the apparent heat shock protein expression coupled with high-intensity expression were separated and raised to later test for heritability of a germline insertion of the injected Cas9 construct. Crossing of a potential F0 fish with a wildtype fish would generally result in normal Mendelian heritability of about 50% of any potential gene construct inserted into the germline of the F0 fish. Embryos resulting from these matings were additionally subjected to the heat shock protocol as an additional method to screen for the heritability of an injected Cas9 construct.

Whole-Mount in Situ Hybridization (WISH)

WISH is a common protocol done to visualize the expression of RNA in embryos using synthetically produced RNA probes. A complementary labeled nucleic acid sequence binds to a specific genetic sequence in the tissue and is visualized using dyes, such as BMPurple or DAB substrate. Because WISH stains where genetic sequences are

expressed rather than the protein itself, WISH can be important for understanding the function of specific genes (Zhang 2013).

Preliminary work is done to design primers from a template such as age-specific cDNA from zebrafish or a plasmid specific to the exact target sequence contained in zebrafish. The genetic template and the primers are run in a PCR to amplify the sequence of choice and then a riboprobe is fabricated (Narayanan 2019). Additionally, zebrafish embryos of the desired time point are fixed overnight, dechorionated, bleached to remove melanin pigment, and dehydrated in increasing concentrations of methanol. Once placed in 100% methanol, embryos are stored in pure methanol overnight at -20°C until the WISH protocol is performed.

The essential steps of WISH include rehydration, incubation of the embryos with the riboprobe, incubation with the antibody, and development of the color signal over three days. An extended step-by-step protocol of WISH can be found here (Thisse 2008). At the end of the protocol, WISH-stained embryos are stored in stop solution (PBST with EDTA) or 100% glycerol prior to imaging.

Cryoembedding and Tissue Sectioning

Embryos that are preserved in a 4% paraformaldehyde (PFA) solution may be prepared for frozen tissue sections for a variety of procedures and further tissue analysis. After removing the PFA solution, the embryos are incubated in a 15% sucrose solution until the embryos sink in solution. Following that, the embryos are incubated in a 30% solution until they are able to sink in solution. An additional incubation in OCT compound (Sakura USA Cat. #4583) will allow for easier embedding of individual specimens in OCT block preparation.

Using a cryoblock mold, OCT compound is used to fill slightly above the halfway fill line of the mold. The target specimen is carefully moved from its incubating solution and positioned toward the center bottom of the liquid contained within the mold. The orientation of the specimen would vary based on the desired plane the user would be intending to section the specimen by. For our purposes, all specimens were placed laterally to obtain sagittal sections of the midline of the embryo.

After positioning the embryo, the block is lowered into a dry ice-chilled bath of methanol to freeze the OCT block until completely frozen, as indicated by the complete color transition from translucent colorless liquid to a fully opaque white color as the OCT compound freezes. The specimens are then stored in a -20°C freezer until ready to be freshly sectioned.

When ready to prepare the fresh frozen sections, a cryostat is equipped with a microtome blade and set between a 0° and 5°-degree angle for the blade. The internal temperature of the cryostat will typically be set between -18°C to -14°C to ensure optimal cutting of the specimen. The prepared block is attached to a metal chuck with additional OCT compound and brought close to the microtome blade before attempting to cut individual sections. Rolls of cut specimen form as the microtome cuts sections and the section rolls are slowly unfurled with the use of specialty paint brushes using delicate and slow even motions. The sections are then placed on the positively charged side of a glass slide. The slides should be stored at -20°C until ready to be further processed.

Hematoxylin and Eosin Staining

Also known as H&E stains, multiple versions of this staining protocol exist, and they are the most performed staining procedures for routine tissue analysis. Hematoxylin

stains nuclei purple-blue while Eosin stains the extracellular matrix and cytoplasm pink. Other structures in the tissue take on different mixes of both stains, allowing the different stains to help distinguish additional details about the tissue. Further details about the mechanism of action and detailed steps of the actual protocol can be found on the official Leica website (Sampias, Rolls 2024).

RNAscope and Confocal Microscopy

RNAscope is an *in situ* hybridization technique that allows for cell-specific expression of specific genes in the spatial context of the tissue itself, which helps with the visualization of gene expression. Multiple genes can be stained for simultaneously in what is called multiplexed RNAscope. Unlike WISH, RNAscope probes are designed in a proprietary manner with Bio-Techne to target genes of interest and optimize the visualization of multiple genes of interest. A paper discussing the use of RNAscope on zebrafish tissue can be found here (Gross-Thebing 2020) while a step-by-step guide for RNAscope can be found on the ACDbio website (RNAscope).

RNAscope is performed on prepared slides of zebrafish embryos and the essential steps of the protocol can be summarized as tissue preparation and pretreatment, probe hybridization to allow the probes to bind to the target RNA, amplification to enhance detection of probe signals, and coverslip mounting with imaging and analysis to follow.

Light Sheet Microscopy

The light sheet microscope allows for live imaging of a developing embryo mounted in an agarose noodle within a prepared glass capillary. Preparation for a light sheet experiment starts with the breeding of embryos to be imaged and timing preparation

1-2 hours before the beginning of the imaging experiment. A glass capillary is cut to allow the insertion of a wire which is used as a plunger to uptake agarose into the capillary. Using a solution of 1% agarose with a lower melting temperature, a heat block is set at 50C to melt the agarose until ready for use. Agarose is dropped onto a flat surface under a microscope and allowed to cool slightly without solidifying.

Embryos are dechorionated and anesthetized with tricaine at a low dose to facilitate mounting and embedding into the agarose. Once within the agarose, the plunger is retracted to embed the embryo into the agarose-containing capillary and then adjusted to partially expose the head of the zebrafish embryo within the agarose but slightly outside the glass capillary. Development of these techniques has shown that zebrafish can tolerate being embedded within agarose for up to 72 hours while continuing to develop regularly (Weber 2014, Kaufmann et al., 2012) Once the zebrafish-containing capillary is prepared, it is held in embryo medium with a low dose of tricaine until ready to be mounted into the microscope.

Microscope preparation involves the microscope's initialization steps, preparation of the imaging chamber, and calibration of the imaging lasers. The chamber must be filled with filtered E3 medium to reduce artifacts from distorting image quality. Additionally, an adequate low dose of tricaine is used to ensure the embryo's comfort and decrease its movement during the imaging process. Calibration of the microscope must occur before mounting the embryo on the system and is done for each fluorophore and every single time the magnification is changed for an experiment. The stage that holds the capillary is raised to the highest placement and the embryo containing the capillary is loaded into the light sheet microscope. Once experimental image capture points are

configured, the experiment is started. Raw light sheet imaging data following the capture of the image time course is processed within the Luxendo imaging processor and can then further be examined with the internal image viewer or the Imaris software suite for further computational analysis.

Chapter III.

Results

WISH Probe Fabrication and Results

Three genes were selected for their connection to expression within the pituitary at various points during the zebrafish's early development and for their specificity to outside anatomical markers for reference . These three genes were *lhx3*, *pomca*, and *pitx3*.

lhx3

lhx3 is expressed throughout the development of the zebrafish starting from the pituitary placodes and later through the development of the hindbrain, spinal cord, and motor neurons. Multiple attempts to fabricate a WISH probe with specific staining, utilizing both fabricated cDNA libraries for zebrafish at various time points and plasmid DNA did eventually yield a probe with faint expression observed in the pituitary placode. (Figure 2 *lhx3* WISH WT) Given the faint staining from the *lhx3* probe within WT fish, we opted not to do further WISH staining for the probe.

pomca

pomca is expressed in both the pituitary and throughout the brain, particularly the hypothalamus from early through later development of motor neurons. Our attempts to create a *pomca* WISH probe were successful with clear and specific staining observed at later time points of development, but not at earlier time points of development. (Figure 3: *pomca* WISH staining WT 4 dpf). This may be because *pomca* may not be expressed in

high quantities at earlier time points of development (Daniocell *pomca*). Previous WISH staining attempts by other labs also show extremely scant staining at 32 hpf in WT embryos (Nica et al., 2006). We experienced substantial difficulties in performing DNA extractions and subsequent fragment analysis on samples that underwent in situ analysis and instead utilized the *pomca* probe's ability to visualize later development of the pituitary when assessing whether use of our morpholino injection was effective in inducing the esrp1/2 mutant phenotype. As shown here (Figure 4 pomca MO test), representative images of WT, *esrp1/2* mutants, and *esrp1/esrp2* MO-induced embryos are shown for side-by-side comparison. These results show WISH staining of pomca within the esrp1/2 mutant that is identical to our esrp1 KO, esrp2 MO-injected embryos. These images contrast with WT embryos at the same stage of development which show much more progression of the posterior movement of the developing pituitary.

To score the effectiveness of the morpholino, we injected two concentrations of morpholino into two groups of *esrp1* mutant embryos to judge if differences in the concentration of morpholino would result in differences for the induction of the *esrp1/2* mutant phenotype or if there would be differences in the survival of either group of morpholino injected embryos. We observed no differences in the survival of embryos among both injection groups. Additionally, we performed WISH on samples of both groups along with controls and took images of each specimen. Each image was scored from a lateral view for of the progression of the posterior movement of the pituitary where the staining of each embryo was given a score between 1 and 0, where a score of 1 indicated normal progression of the posterior movement and development of the pituitary and 0 indicated severe delay in this expected posterior movement. We scored both

morpholino groups the same in terms of the ability to induce the *esrp1/2* phenotype at about 90% effectiveness with no notable die-off of WISH specimens prior to preparation for *in situ*. A summary of that scoring can be found in Table 1 (Scoring of Morpholino Effectiveness).

pitx3

We were successful in generating a *pitx3* probe and were able to achieve clear and specific staining through early development of the pituitary placodes. (Figure 5 *pitx3* WT 24 hpf) WISH staining at 24 hours and subsequent time points revealed the rapid nature during which the placodes merge and eventually migrate backward from the anterior midline of the face toward the posterior of the head. We additionally observed differences in development between WT and mutant cohorts in their ability to organize cohesive movement of the placodes at the same time points (Figure 6 *pitx3* 28 and 30 hpf). We also observed that morpholino-injected mutants from both time points exhibited additional segmentation of the pituitary placodes as well as observed delay as compared to the progression of development observed from both control morpholino-injected embryos and normal WT embryos from the same time points. From the overall series of *pitx3* WISH staining, we were able to determine that the optimal developmental time points to observe the placodal movement in a posterior direction would be optimal starting from 30 hpf.

RNAscope 4 dpf WT and *esrp*1/2 mutant

Sections of 4 dpf embryos were prepared of the midline of each specimen following instructions outlined for cryopreservation of embryos and preparation of frozen sections. We designed Multiplexed RNAscope probes for three channels for *esrp2*, *lhx3*,

and *pomca* to visualize the location and normal development of the pituitary within typical wildtype embryos. Minor modifications were made to the target retrieval portions of the protocol with no other notable deviations from the ACDbio-provided protocol for RNAscope. Figure 7 shows a compound image of the results. *esrp2* was set as channel 1 using the Opal 570 dye pseudo-colored in the image as magenta. *lhx3* was set as channel 2 using the Opal 690 dye and was set to be pseudo-colored as yellow. *pomca* was set as channel 3 using the Opal 520 dye and was pseudo-colored as green. With the section of the embryo facing to the left, *lhx3* is notably visible in two locations which correspond to the epiphysis at the top anterior portion of the head and the developing pituitary. Both locations have had circles added to them to bring focus to their anatomical locations. In addition to *esrp2*'s normal expression throughout the epithelium, *esrp2* is shown to localize with *lhx3* at both noted locations. *pomca* expression is also noted in conjunction with *lhx3* and *esrp2* expression around the pituitary.

Generation of an *lhx3* Transgenic Fishline

We injected upwards of 500 embryos with an *lhx3:tdTomato* Cas9 guide following methods outlined concerning the injection of embryos. These embryos were subjected to a heat shock protocol to do an initial screening to see whether the Cas9 construct was inserted into the embryos' genome (Figure 8: heat-shocked embryos). Embryos displaying both high-spread expression and high-intensity expression of the heat shock protein were raised until breeding age and then fin clipped to analyze whether the construct was expressed in the grown fish's tissue (Figure 9: gel testing for tdTomato in grown f0). Fish showing positive expression of tdTomato from their fin clip DNA were then set up in breeding pairs to test whether their embryos were both able to be

ordinarily screened for fluorescence and whether these embryos would display heightened fluorescence after also being subjected to the heat shock protocol. Positive expression of the fluorophore from the heat shock promoter would further indicate the insertion of a Cas9 construct in the germline of the injected parent fish.

Exposure of the embryos from one of our injected fish did result in an inducible heat shock fluorescent signal from a large portion of embryos among those laid (Figure 10). We later screened another clutch of embryos from the same fish for inherent expression of the fluorophore and took images of its endogenous fluorescence at three different time points (24 hpf, 48, hpf, and 5 dpf) and compared them to existing WISH staining from literature (figure 11 *lhx3:tdTomato* comparison), where it was observed that there was an apparent match of the expected expression between both sets of data. We especially note the signal apparent at the location of the pituitary, most notably at the 24 and 48 hpf time points.

DNA extraction was performed on potential F1 embryos exhibiting endogenous expression of the fluorophore using primers for *lhx3* and a site related to the heat shock promoter. We identified an expected gene product of approximately 300 bp for each of the embryo pools from which DNA was extracted (Figure 12 F1 embryos *lhx3*-hsp PCR product). We performed a temperature gradient on the DNA sample from the first lane of our previous gel and found the optimal annealing temperature to be 57°C resulting in fewer off-target gene products. Optimized PCR samples were sent for Sanger sequencing for confirmatory genotyping of the F1 embryos. The sequencing results are laid out in Figure 13 (*lhx3* F1 Sanger sequencing). There was an observed deviation from the normal expected Mendelian expression of the transgene which is laid out in Table 2 (Transgene

expression tally among F1 embryos). We did additional PCR analysis to see if we observed the same gene products observed in positive screened embryos were present in the visually screened negative embryos to test those embryos in the F1 clutch still had the construct, (Figure 14 Negative screened F1 embryo PCR analysis) and found several additional embryos with the gene product that was described earlier.

Light sheet microscopy

We attempted to visualize pituitary development through different reporter lines, most notably with the *lifeact:gfp* line crossed with *shh:rfp*. *Lifeact* has frequently been used in several biology disciplines to visualize the beta-actin structures within eukaryotic cells and is used as a universal imaging marker (Riedl 2008). Because placodes are defined as a thickening of the endoderm or ectoderm, we expected a heightened beta-actin signal to help locate the developing pituitary. *Shh* was chosen for its ability to visualize the hypothalamus, mesoderm, and the central nervous system which were intended to serve as anatomical reference points. We captured a time course of development from about 30 hpf to 40 hpf following our methods involving the setup of light sheet experiments. A still image of our experiment can be shown from the lateral view in Figure 15. From this, we were able to visualize the location of the pituitary placode as being situated at the base of the head above where the yolk sac begins. Figure 16 shows where this location is from lateral frontal and dorsal views by utilizing the Imaris orthogonal slicer. Both unobstructed views and crosshairs are aligned across the three views to show the exact anatomical position we observed increased *lifeact:gfp* signal from. Over the span of the experiment, we note the movement of the identified placodal signal in a posterior direction toward the hypothalamus over the next several

hours. Additionally, we note the visible inward convergence of epithelium in conjunction with the posterior movement of the pituitary placode originating from both the head and the yolk.

Chapter IV

Discussion

Evaluation of the *lhx3:tdTomato* transgenic line

Potentially Lethal Knockout of *lhx3*

One possible drawback of propagating this transgenic line is that the action of incrossing screened positive embryos to create a homozygous expression of lhx3: tdTomato may result in a homozygous mutant lethal phenotype. In mice, loss of both *lhx3* alleles results in a lethal phenotype (Netchine et al. 2000). The insertion of a large CRISPR Cas9 construct, while enabling visualization of the development of the pituitary, effectively knocks out the expression of one of the normal alleles. Observation of F1 embryos expressing the fluorophore to this point has not been tied to detrimental effects in their normal development likely suggesting that zebrafish are able to tolerate loss of a single copy of *lhx3* while still expressing the gene construct.

Notably, not all genes that are lethal in mice or other animal models are always lethal in the zebrafish model, such as is the case with *Ersp1* when compared among zebrafish and mouse study models (Carroll et al. 2020, Yang et al. 2016). Given this, it may be possible that other genes such as *lhx4* may compensate for the loss of *lhx3* but the evaluation of lethality of the homozygous expression of *lhx3:tdTomato* would be beyond the scope of this thesis project.

Deviation from Mendelian ratio of Observable Fluorescence

As mentioned previously there was not an observed Mendelian ratio of offspring in the F1 generation of embryos. Table 2 shows statistics performed on the numbers of observed embryos among 100 random individual F1 embryos in comparison to the number of embryos that should be expected to express the transgene (Mendelian inheritance, null hypothesis) and the actual number observed among each plate as well as the additional numbers of embryos that were later screened as positive following DNA extraction and analysis of PCR products on gel through figure 14. On average only around 25% of the expected number of embryos were able to be visually screened positive among each plate of fish. For both sets of visually screened positive (12) and screened positive along with PCR positive individuals (30), both numbers fell outside of the 95% confidence interval to be classified as having normal Mendelian inheritance, indicating rejection of the null hypothesis.

One possible explanation for this may be because the insertion of a large CRISPR Cas9 construct exceeds the normal distance a gene may typically be located from its promoter region. Typically, promoter regions lie around 10-1000 base pairs away from the gene sites they amplify with greater base pair distance resulting in reduced translation and transcription (Addgene: Promoters). By comparison, the inserted Cas9 construct for the heat shock promoter precedes the tdTomato construct in the sequencing data and creates a gap of over 1400 base pairs difference from the normal location of the wildtype *lhx3* gene which may affect the promoter region's ability to promote *lhx3:tdTomato* expression in any F1 embryo. This likely means that expression of tdTomato may only occur if the promoter region can properly promote transcription of the tdTomato fluorophore, which is not tied to Mendelian inheritance of the CRISPR Cas9 construct.

Another possible explanation for the deviance from expected Mendelian ratios is that the gene construct order of the heat shock promoter upstream of tdTomato may impede expression of tdTomato due to a compound restriction enzyme site containing a stop codon, meaning that cell machinery may not transcribe additional gene products after this stop codon. This may be a reason why additional embryos with the identical gene construct could be identified by both heat shock protocol and through DNA extraction despite not endogenously expressing the tdTomato fluorophore.

Public Health Implications

As previously discussed, options to visualize pituitary development were limited to techniques involving the sacrifice of study animals or in vitro models that would not allow for observation of growth deficiency effects in other parts of the study organism. With the creation of an *lhx3* reporter, it is possible to visualize pituitary development distinctly tied to the expression of a key pituitary marker in a study model that allows for live imaging to show real-time development of the pituitary's normal development. This transgenic line was developed to visualize differences in pituitary development in relation to normal and affected development because of compound mutations in both *esrp1* and *esrp2* for future grant-funded research, but the research applications could extend beyond the scope of those projects as well.

Additionally, the relation of *esrp1* and *esrp2* mutations to both craniofacial disorders and its possible connection to pituitary disorders may have implications for what symptoms and diagnoses patients may receive when being screened for either health issue. Because of the plausible connection to compound *esrp1/2* mutations, steps have been taken by our lab to identify patients with the coincidence of both craniofacial

developmental symptoms and endocrine syndromes with plans for our lab to correlate the two in human patient populations.

Conclusion and Future Directions

Through the various experiments completed for this project, we were able to confirm our hypothesis of being able to visualize differences in pituitary development within the zebrafish study model including both early development prior to merging of two separate pituitary placodes and later development in accessing the extent to which mutations in *esrp1* and *esrp2* may impede its development. Our findings support theories of pituitary placodal development from two distinct pituitary placodes which merge around 27 hpf and the merged pituitary placodes' migration posteriorly until its eventual development into the mature pituitary. Additionally, we created a transgenic line tied to a key protein within the developing pituitary, *lhx3*, that may be useful in further visualizing the notable differences in pituitary development within *esrp1/2* mutant embryos that will help our lab further investigate their role as a causative factor for both craniofacial malformations and endocrine disorders

Appendix

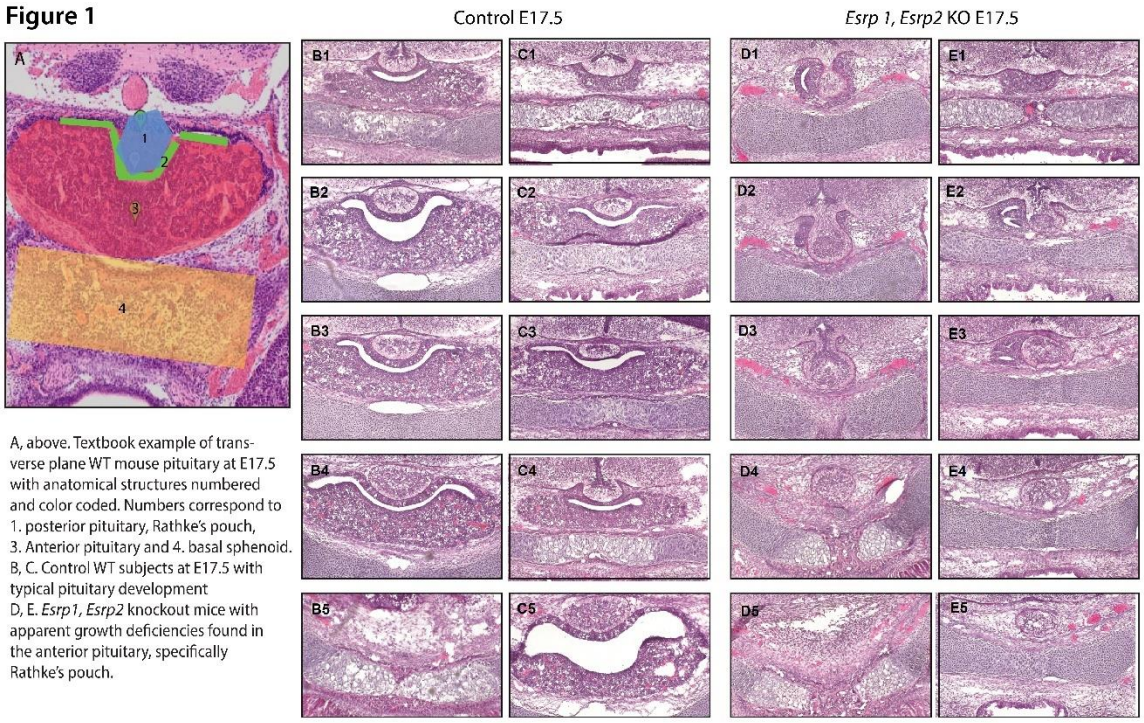

Figure 1: *Esrp1/2* mutant embryos' pituitary development at E17.5.

Section A shows a section of a typical pituitary for mice at the 17.5E stage of embryonic mouse development with notable anatomical regions highlighted by colored regions. The notable anatomical regions include the posterior pituitary (1), Rathke's pouch (2), the anterior pituitary (3), and the sphenoid bone (4) which serves as an anatomical landmark. Sections B-C Two mice with subsequent sections provide a view of the developing pituitary within wildtype mice. D-E Two mice with subsequent sections provide a view of the developing pituitary within Esrp 1/2 knockout mice. The notable differences to note between both phenotypes are the lack of invagination of Rathke's pouch and the failure of the anterior pituitary to form and proliferate.

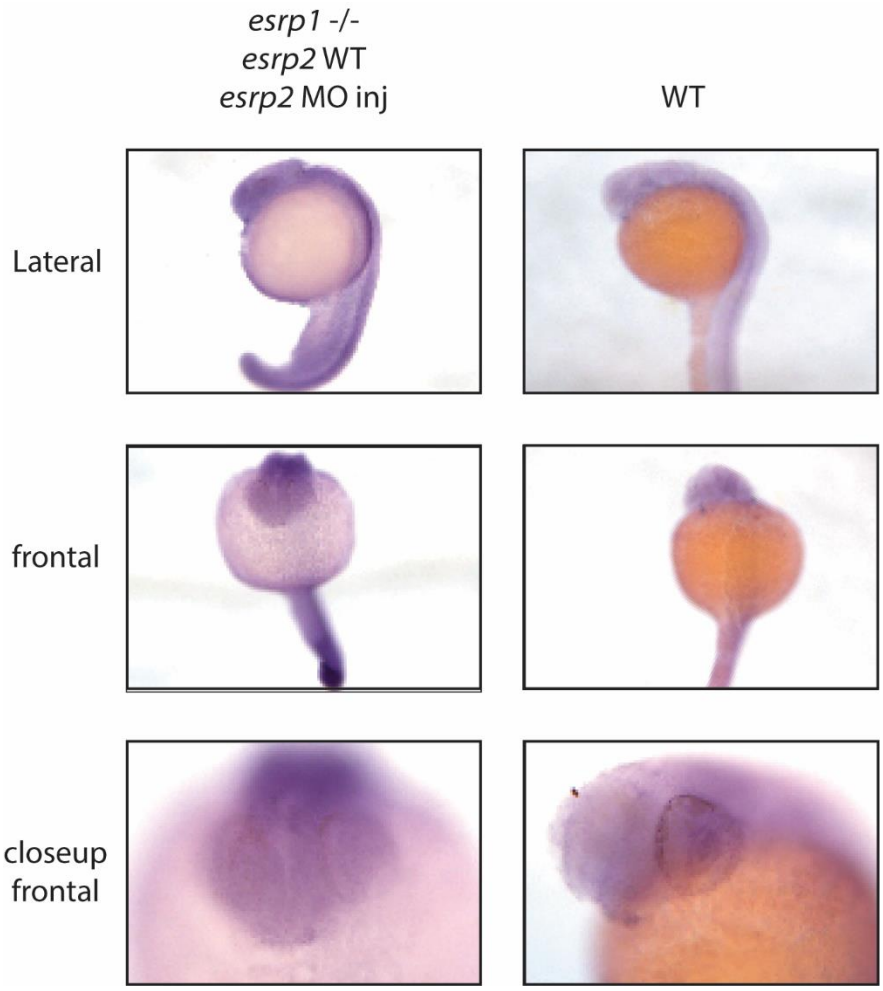

Figure 2: *lhx3* WISH Staining at 24 hpf

Multiple attempts were made to design and visualize the expression of lhx3 within embryos at the 24 hpf stage of development. Here we show the results of a whole mount in situ with apparent but low staining signal. Reasons for this are likely due to the low expression of lhx3 at the beginning of pituitary placode formation and prior to the merging of preliminary placodal tissue at this stage of development. Differences between the two groups appear to be a delay in the convergence of the apparent pituitary placodes

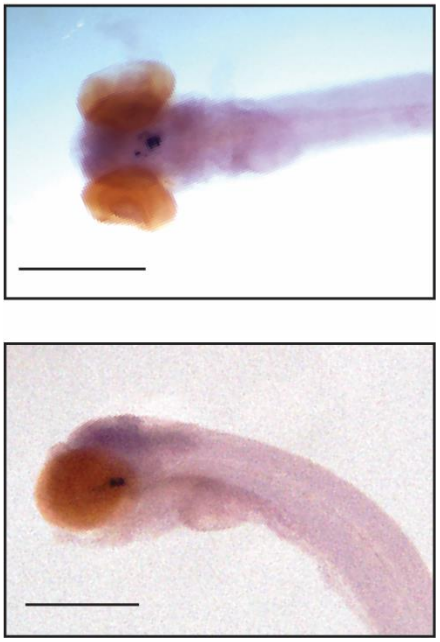

Figure 3: *pomca* WISH staining on WT at 5 dpf

pomca WISH probe staining performed on WT 5 dpf embryos. We attempted to visualize pomca staining at earlier stages but were unable to generate images for our earlier time points likely due to its activation in later stages of embryonic development. pomca was helpful for visualizing the posterior movement of the merged pituitary placodes in the later development of the pituitary.

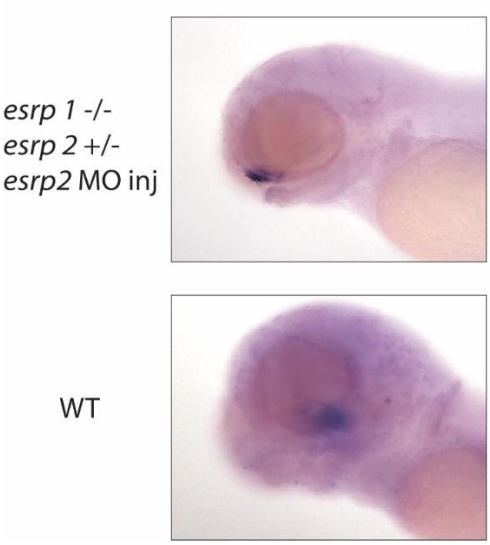

Figure 4: *pomca* 4 dpf WISH staining on WT and *esrp1/2* MO-injected embryos

Morpholino was injected into esrp1 KO, esrp2 heterozygote embryos to ensure complete knockdown of both esrp1 and esrp 2. To ensure that the phenotype was consistent with what we expect for esrp double knockouts, we took images of over 20 specimens per test group and scored them (0 to 1) based on the level of posterior movement the pituitary was able to make over the individual embryo's development. Morpholino-induced esrp double knockout fish showed significant delays to the expected posterior movement of the merged pituitary placode as opposed to the expected posterior movement of the merged placode within wildtype embryos.

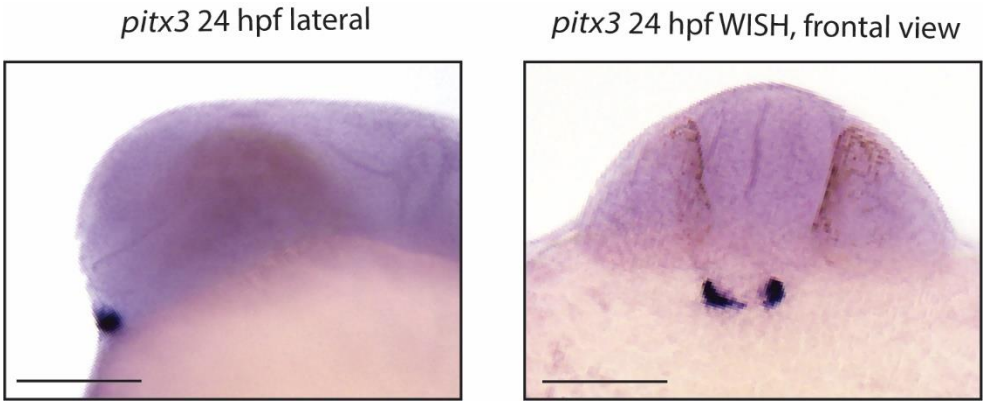

Figure 5: *pitx3* WISH 24 hpf WT

pitx3 WISH staining on 24 hpf wildtype embryos. Among the genes we attempted WISH on, pitx3 showed the clearest staining with the strongest signal among 24 hpf WT embryos. A clear strong signal is apparent from the location of the pituitary placodes at the base of the head before the merging of the two distinct pituitary placodes.

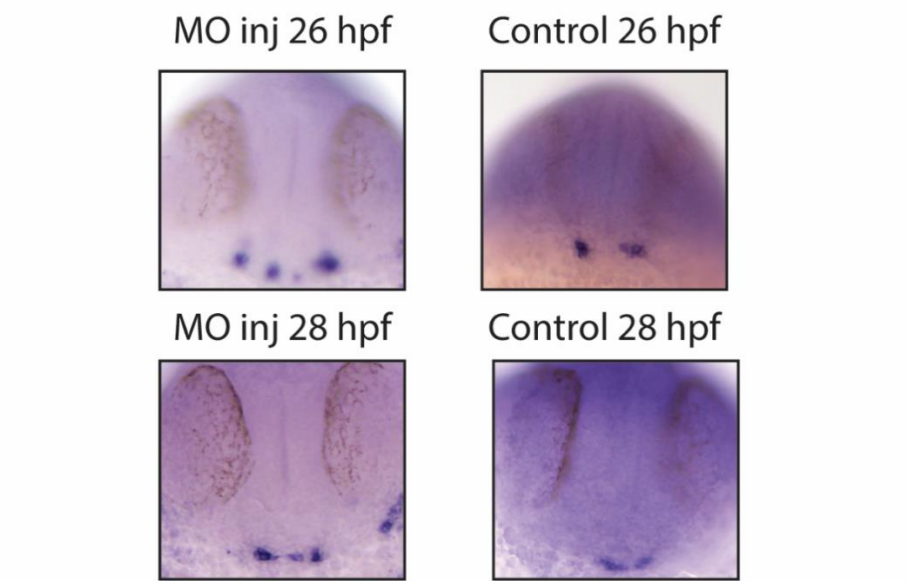

Figure 6: *pitx3* WISH for 26 and 28 hpf WT and morpholino injected

esrp1 knockout embryos were injected with the esrp2 morpholino to increase the incidence of an esrp1 and 2 compound knockout phenotype. The embryos underwent WISH for two different time points and were compared to wildtype embryos at the same time point for differences in expression. Esrp1/2 knockout fish phenotypically exhibit both delay and less cohesive migration of the developing pituitary placodes as opposed to wildtype fish at the same point in development.

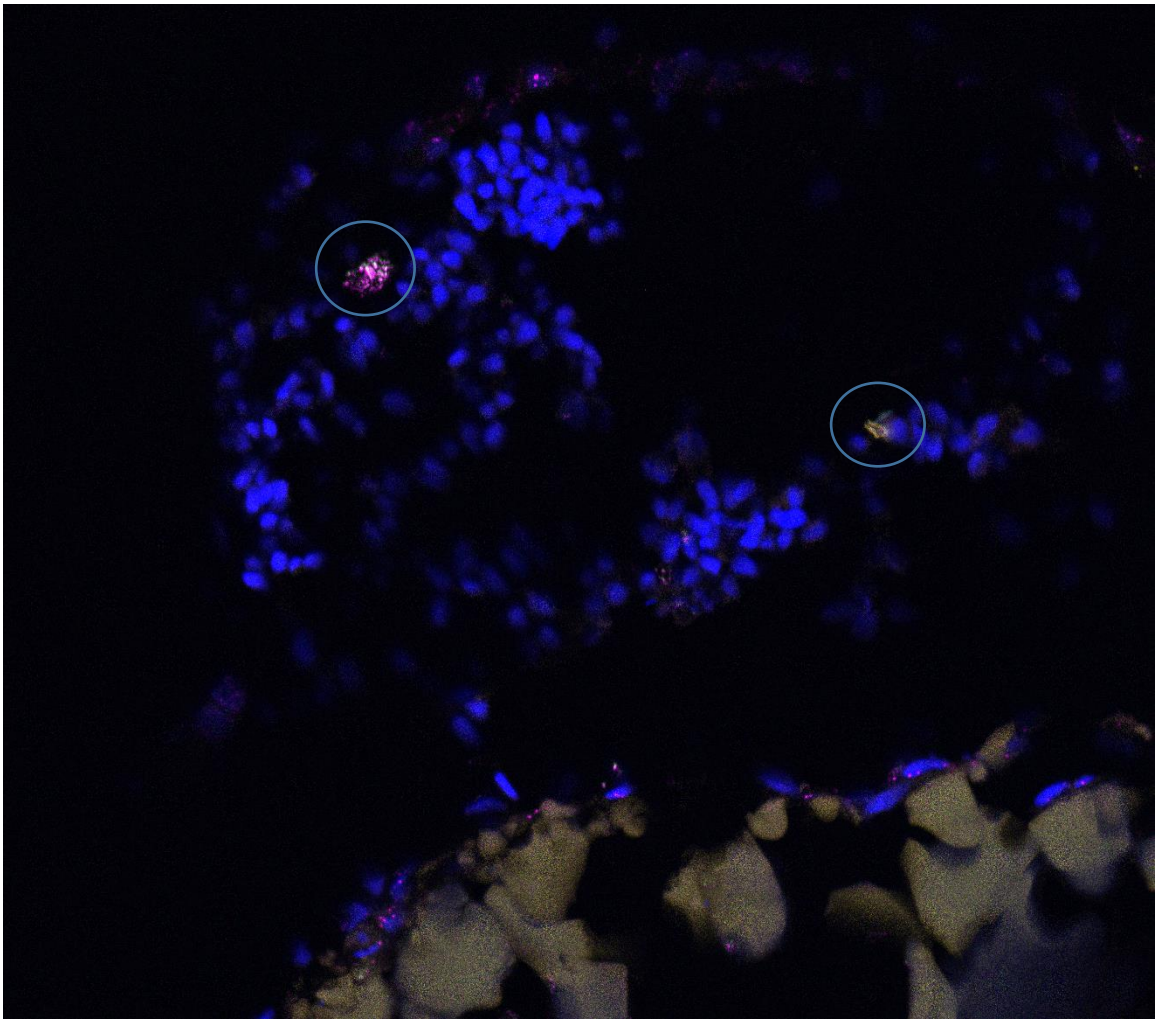

Figure 7: RNAScope 4dpf W*T*

Shown above are the compound image results of multiplexed RNA scope performed on a wildtype 4 dpf embryo through the midline of the specimen. Esrp2 is magenta, lhx3 is yellow, pomca is green. Lhx3 is notably visible in two locations which correspond to the epiphysis at the top anterior portion of the head and also the developing pituitary. Both locations have had circles added to them to bring focus to their anatomical locations. In addition to esrp2's normal expression throughout the epithelium, esrp2 is shown to localize with lhx3 at both noted locations. pomca's expression is also noted in conjunction with lhx3 and esrp2 expression around the pituitary.

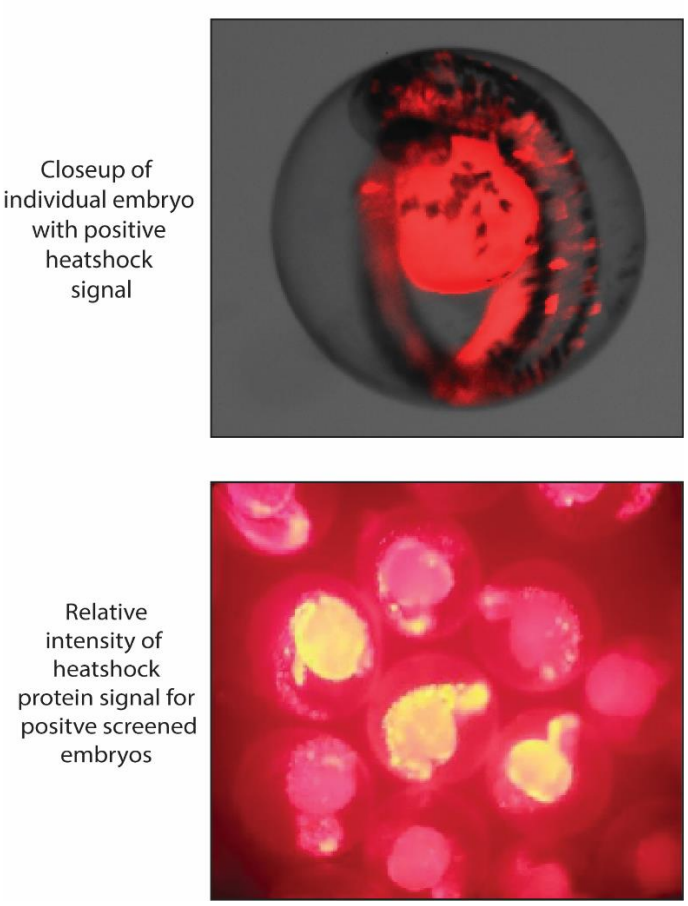

Figure 8: Heat-shocked injected embryos

The images show embryos 24hpf following the injection of a lhx3 CRISPR Cas9 injection guide. The purpose of the injection was to introduce a fluorophore tied to the expression of the lhx3 gene which is expressed starting from the beginning of placodal development and up through the complete maturation of the complete pituitary organ. The lhx3 guide also introduces a heat shock promoter which can be used to screen for guide efficiency in any individual embryo. Embryos with the highest intensity were screened and raised as high heat shock promoter activity is correlated with a higher likelihood of construct insertion into the germ line of the embryo.

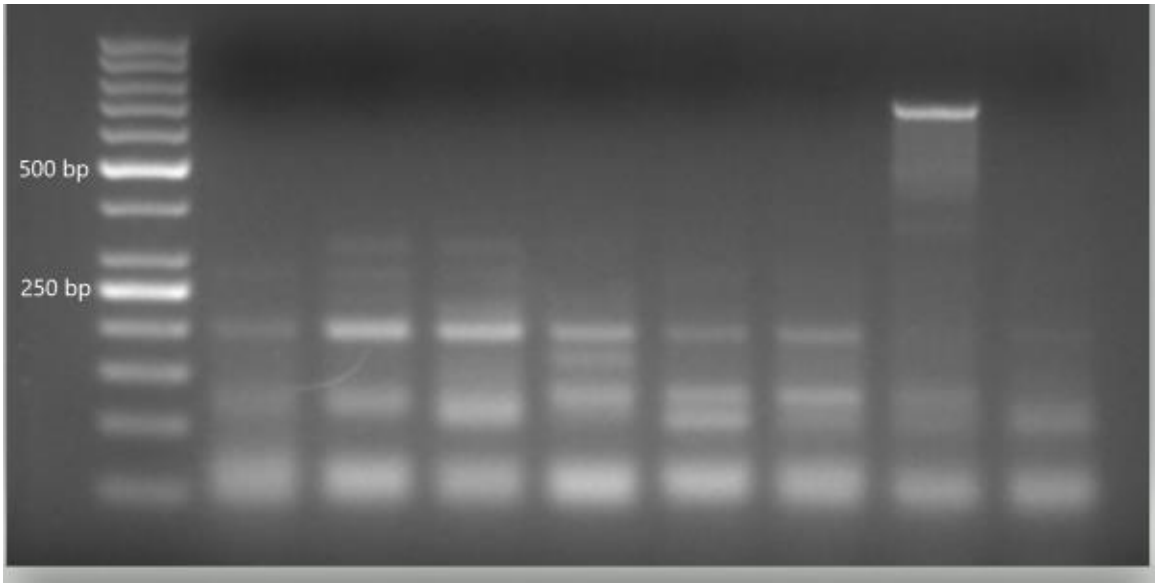

Figure 9: Gel Image for tdTomato PCR product from F0 fin clip DNA extraction

Here is an example of a gel that was done on lhx3:tdTomato guide injected embryos that were raised to adult age and fin clipped to test for a tdTomato PCR product. The seventh lane shows a positive example of a fish that would be considered positive for a tdTomato PCR gene product. The expected PCR product is about 700 base pairs from the genotyping primers that were designed. Fish that were identified as having the tdTomato PCR product were kept on the aquatic system to later test for a heritable germline insertion of the lhx3:tdTomato construct among their embryos.

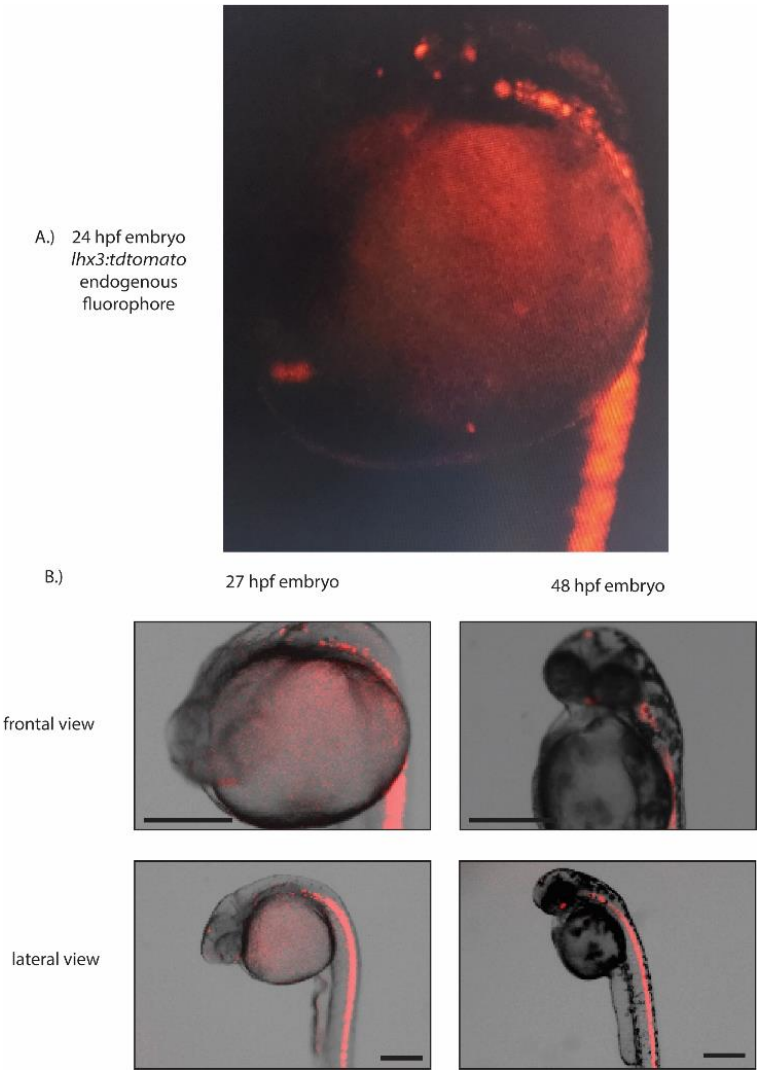

Figure 10: F1 *lhx3* embryo time course showing merging of pituitary placodes

Part A shows a 24 hpf lhx3:tdTomato F1 embryo with two distinct visible fluorophore signals located at the front base of the embryo's head. The fluorophore signal is isolated from the transmitted light portion of the image to aid in visibility of the two distinct and separate placodes prior to their merging. In part B, we show a 27 hpf embryo as the two placodes begin to merge around 27 to 30 hpf and show in a 48 hpf embryo that these placodes have fully merged and begun their posterior movement toward its final location at the base of the hypothalamus.

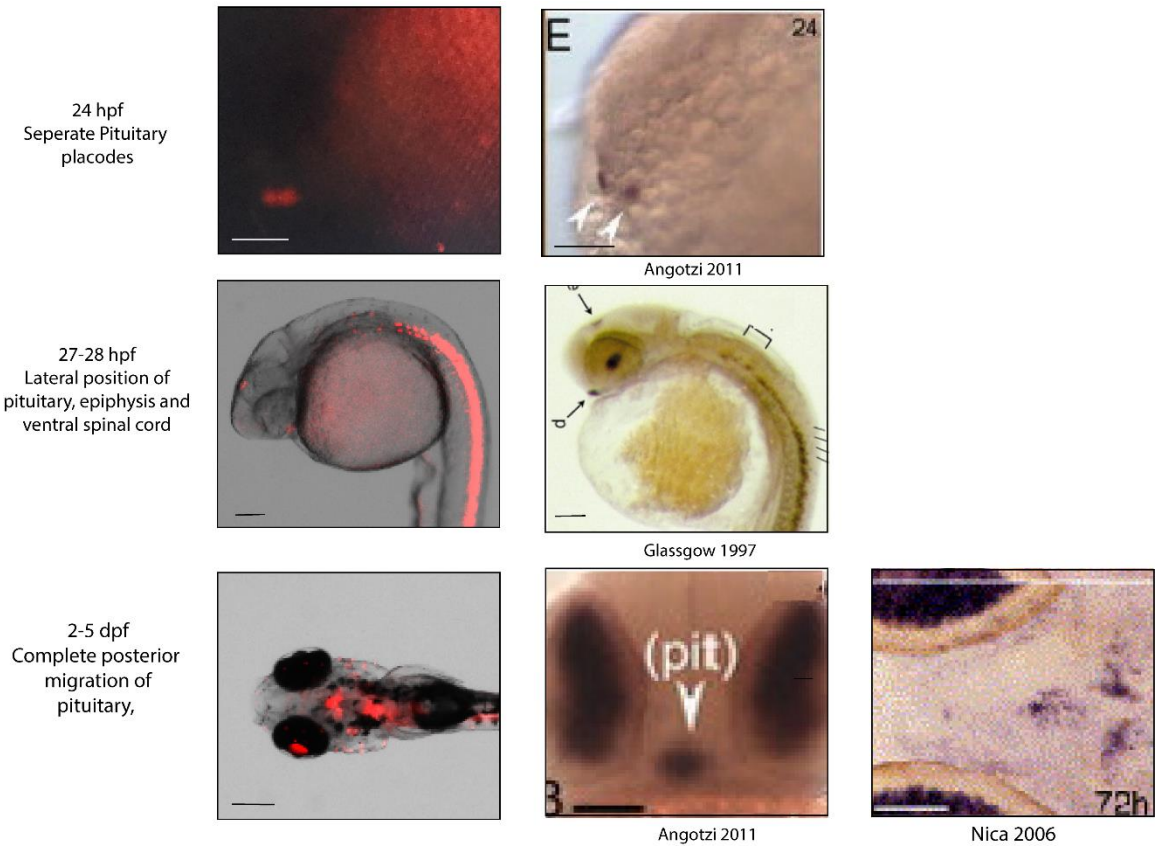

Figure 11: F1 Comparison of *lhx3:tdTomato* images to WISH literature

We compared our captured images to existing wish literature. In the first row, we note the presence of two distinct pituitary placodes visible at 24 hpf. In the second row, we note the apparent fluorescence around the spinal cord as well as the same lateral locations of both the pituitary placode and the epiphysis at the top of the head, which would correspond to staining as noted by the top arrow in the reference image to the right (Glassgow 1997). In the third row, we present a 5dpf embryo in contrast to two referenced images to the right. We note the signal of lhx3 within the retinas of the embryo which arise starting from 2dpf and up through 6dpf according to multiple sources. We additionally note the proliferation of lhx3 signal posterior to the eyes indicating the final location of the pituitary following its posterior movement toward the hypothalamus from 28 hpf to 3 dpf.

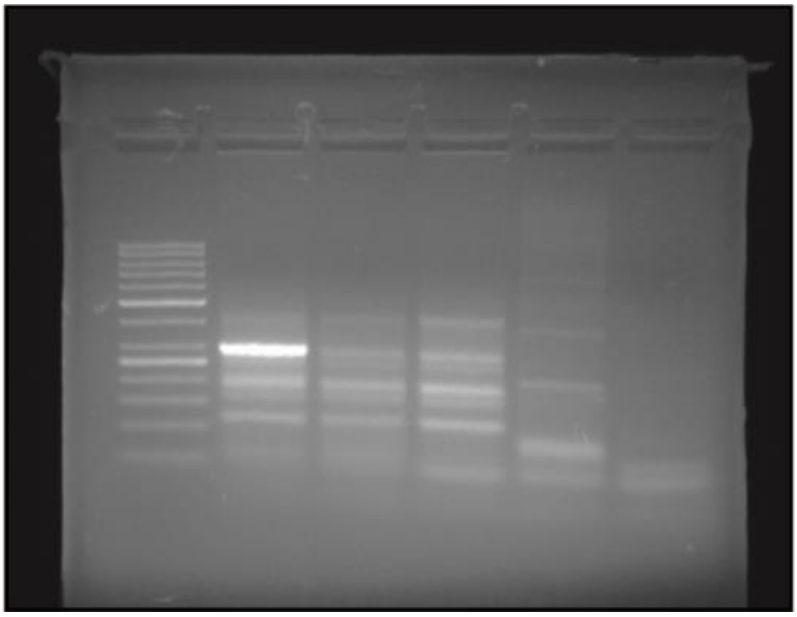

Figure 12: F1 embryos *lhx3*-heatshock promoter gel product

Using a 50-base pair ladder, gel electrophoresis was performed following DNA extraction on three embryos that were screened positive for what is suspected to be tdTomato tied to the expression of lhx3. The first three lanes of the gel show varying intensities for a unique gene product of approximately 300 base pairs that is not present within the two control lanes of the tdTomato plasmid alone and a WT embryo (lanes 4 and 5). The PCR was run using a forward primer for our lhx3 WISH probe and a reverse primer for the heat shock promoter.

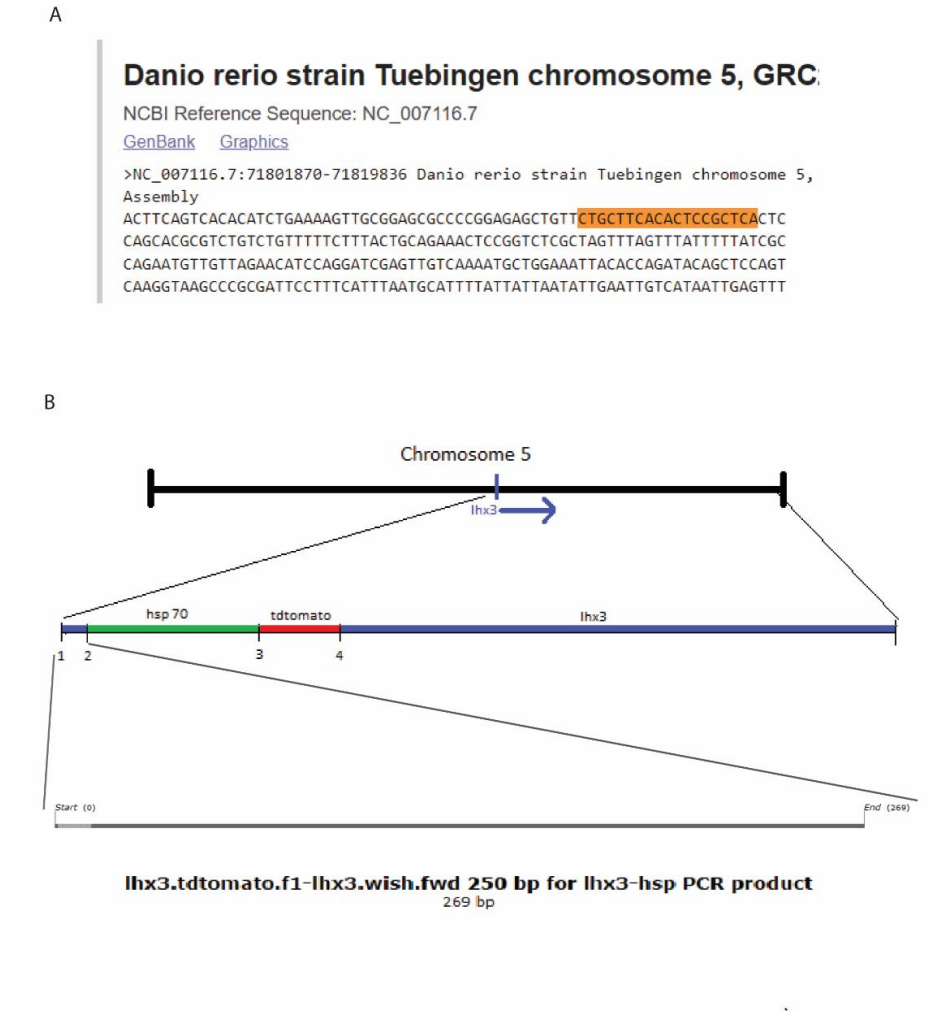

Figure 13: Sanger sequencing of the *lhx3*-heatshock promoter gene construct

Figure 13 DNA extract from F1 embryos was sent for Sanger sequencing. We identified the start site of the CRISPR Cas9 insertion based on the known sites of primers used to genotype for the construct containing the heat shock promoter. The schematic visually shows how close to the beginning of the lhx3 assembly the construct was inserted into. Part B gives a visual idea of what the gene map of the modified lhx3 allele may look like.

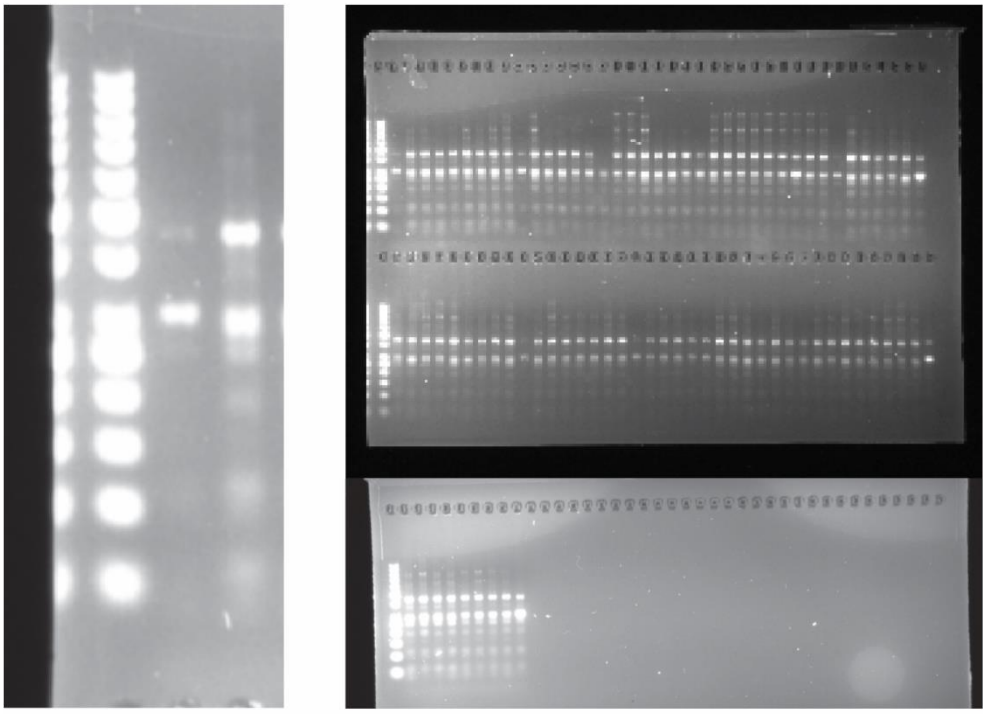

Figure 14: Gel for screening negative embryos for *lhx3*-hsp PCR product

We imaged individual DNA extractions of embryos that were screened as visually negative for the lhx3:tdTomato fluorophore signal. On the left we have our gene ladder followed by an example of an individual that was screened as positive for the PCR product on an agarose gel, followed by a lane that is negative for the target PCR product. Out of 100 embryos, 16 were screened as visually sorted positive (saved and raised on the aquatic system) and N=84 embryos were tested through PCR for the lhx3-heatshock promoter gene product. Out of 84 individuals, an additional 18 were screened as potentially having the 300 bp target gene product previously identified. Testing of the null hypothesis of Mendelian inheritance is explored in Table 2 using these numbers.

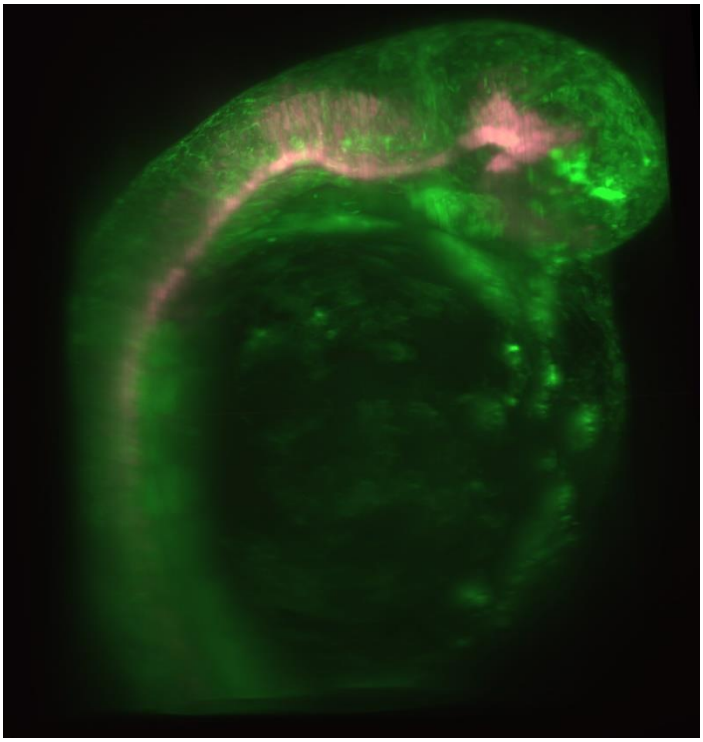

Figure 15: lateral view of *lifeact gfp* x *shh rfp* in Luxendo light sheet image viewer

The Luxendo image viewer is internal software used to view independent fluorophore channels captured using the light sheet microscope. We were able to visualize the internal structures of a developing zebrafish embryo expressing two different fluorophores. The embryo in this figure is an embryo resulting from a cross between a gfp:lifeact, beta-actin transgenic fish and an rfp: shh transgenic fish. Shh was chosen to act as a landmark for the hypothalamus relative to the proliferation and migration of cell clusters as made visible by the signal strength of the beta-actin signal.

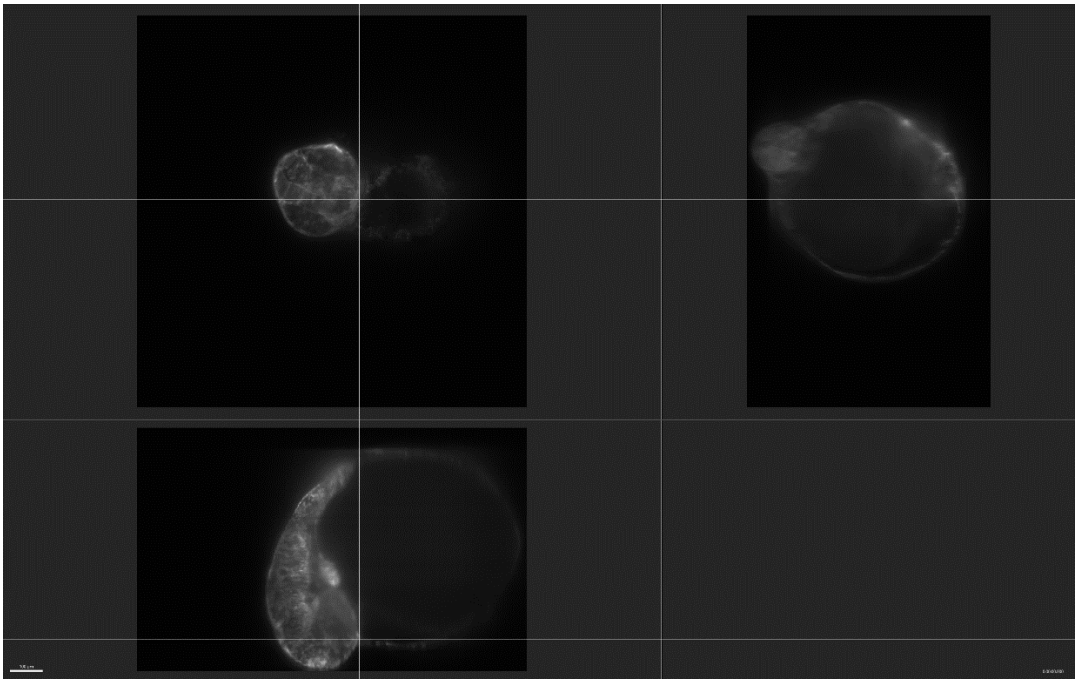

Figure 16 Orthogonal projection views of pituitary in 30 hpf *lifeact* x *shh* embryos

The Imaris viewer helped us individually analyze single channels of each fluorophore's signal. By using the orthogonal viewer function to view the expression of the gfp: lifeact signal we can pinpoint an exact location within a 30 hpf embryo where the merged pituitary placode lies at this time of development. The above image displays a frontal, lateral, and top-down view along with faint white lines that help show the relative location of a single point compared to the other views.

	Group 1, 1x injected N =21	group 2, 2x injected N=22	Control inj. N = 18
Individuals scored 0 for Normal development	2	2	17
Individuals Scored 1 for impared development	19	20	1
Average score for each experimental group	90.4%	90.9%	5.5%

Table 1: Use of *pomca* WISH probe to test morpholino effectiveness

Table 1 Scoring of individual embryos was performed on ersp1 knockout mutants that were injected with an ersp2 morpholino to ensure a higher likelihood of observing compound mutant phenotypes resulting from the knockdown of both esrp1 and esrp2. To evaluate the effectiveness of the morpholino, each embryo was assigned a score from 0, indicating normal pituitary development, to 1, indicating a notable delay in the expected posterior movement of the pituitary placode. A control MO injection of random primers was used to make sure that any delays in development were not a result of possible injection injury.

Negative screened embryos are scored as 0 and positively screened embryos are screened as 100.

Statistic Type	Sample Clutch Visually Positive	Null Hypothesis
Sample Size N	100	100
Sum	1200	5000
Mean	12	50
Variance, s^2	1066.666	2500
Standard deviation	32.6599	50
Test Statistic	-7.6	0
Standard error of the mean	3.26599	5
Confidence Interval, 95%. 1.96 SD		50 +/- 9.8
Confidence Interval, 99%. 2.576 SD		50 +/-12.88
Confidence Interval, 99.9% , 3.291 SD		50 +/-16.455
Confidence Interval, 99.99%, 3.891SD		50 +/-19.455

Statistic Type	Clutch visually positive+PCR positive	Null Hypothesis
Sample Size N	100	100
Sum	3000	5000
Mean	30	50
Variance, s^2	1600	2500
Standard deviation	40	50
Test Statistic	-4	0
Standard error of the mean	4	5
Confidence Interval, 95%. 1.96 SD		50 +/- 9.8
Confidence Interval, 99%. 2.576 SD		50 +/-12.88
Confidence Interval, 99.9% , 3.291 SD		50 +/-16.455
Confidence Interval, 99.99%, 3.891SD		50 +/-19.455

Table 2: Null Hypothesis testing for lhx3 Mendelian inheritance

Table 2 shows null hypothesis testing based on the number of embryos that were screened positive in both visually screened positive plates and then additional embryos screened as positive through DNA extraction and identification of the lhx3-hsp70 gene product. In both instances, both numbers of embryos identified out of 100 embryos did not fall within the expected ratios of embryos expected from typical Mendelian inheritance.

References

Addgene: Promoters. (n.d.). Retrieved January 26, 2024, from https://www.addgene.org/mol-bio-reference/promoters/

Adenohypophysis. (n.d.). Kenhub. Retrieved February 23, 2024, from https://www.kenhub.com/en/library/anatomy/adenohypophysis

Alternative Splicing. (n.d.). Retrieved February 23, 2024, from https://www.genome.gov/genetics-glossary/Alternative-Splicing

Angotzi, A. R., Mungpakdee, S., Stefansson, S., Male, R., & Chourrout, D. (2011). Involvement of Prop1 homeobox gene in the early development of fish pituitary gland. *General and Comparative Endocrinology*, *171*(3), 332–340. https://doi.org/10.1016/j.ygcen.2011.02.026

Ariel, P. (2017). A beginner's guide to tissue clearing. *The International Journal of Biochemistry & Cell Biology*, *84*, 35–39. https://doi.org/10.1016/j.biocel.2016.12.009

Bebee, T. W., Park, J. W., Sheridan, K. I., Warzecha, C. C., Cieply, B. W., Rohacek, A. M., Xing, Y., & Carstens, R. P. (2015). The splicing regulators Esrp1 and Esrp2 direct an epithelial splicing program essential for mammalian development. *eLife*, *4*, e08954. https://doi.org/10.7554/eLife.08954

Bosch i Ara, L., Katugampola, H., & Dattani, M. T. (2021). Congenital Hypopituitarism During the Neonatal Period: Epidemiology, Pathogenesis, Therapeutic Options, and Outcome. *Frontiers in Pediatrics*, *8*, 600962. https://doi.org/10.3389/fped.2020.600962

Carroll, S. H., Macias Trevino, C., Li, E. B., Kawasaki, K., Myers, N., Hallett, S. A., Alhazmi, N., Cotney, J., Carstens, R. P., & Liao, E. C. (2020). An Irf6-Esrp1/2 regulatory axis controls midface morphogenesis in vertebrates. *Development*, *147*(24), Article 24. https://doi.org/10.1242/dev.194498

Chapman, S. C., Sawitzke, A. L., Campbell, D. S., & Schoenwolf, G. C. (2005). A three-dimensional atlas of pituitary gland development in the zebrafish. *Journal of Comparative Neurology*, *487*(4), 428–440. https://doi.org/10.1002/cne.20568

Cox, L. L., Cox, T. C., Moreno Uribe, L. M., Zhu, Y., Richter, C. T., Nidey, N., Standley, J. M., Deng, M., Blue, E., Chong, J. X., Yang, Y., Carstens, R. P., Anand, D., Lachke, S. A., Smith, J. D., Dorschner, M. O., Bedell, B., Kirk, E., Hing, A. V., … Roscioli, T. (2018). Mutations in the Epithelial Cadherin-p120-Catenin Complex Cause Mendelian Non-Syndromic Cleft Lip with or without Cleft Palate. *The American Journal of Human Genetics*, *102*(6), Article 6. https://doi.org/10.1016/j.ajhg.2018.04.009

Cullingford DJ, Siafarikas A, Choong CS. Genetic Etiology of Congenital Hypopituitarism. (Updated 2023 Feb 5). In: Feingold KR, Anawalt B, Blackman MR, et al., editors. Endotext (Internet). South Dartmouth (MA): MDText.com, Inc.; 2000-. Available from: https://www.ncbi.nlm.nih.gov/books/NBK586145/

Developmental mechanism - axes formation. Embryology. (n.d.). https://embryology.med.unsw.edu.au/embryology/index.php/Developmental_Mechanism_-_Axes_Formation

Doss, M. X., & Sachinidis, A. (2019). Current Challenges of iPSC-Based Disease Modeling and Therapeutic Implications. *Cells*, *8*(5), Article 5. https://doi.org/10.3390/cells8050403

Fabian, P., Tseng, K.-C., Smeeton, J., Lancman, J. J., Dong, P. D. S., Cerny, R., & Crump, J. G. (2020). Lineage analysis reveals an endodermal contribution to the vertebrate pituitary. *Science (New York, N.Y.)*, *370*(6515), Article 6515. https://doi.org/10.1126/science.aba4767

Fang, Q., George, A. S., Brinkmeier, M. L., Mortensen, A. H., Gergics, P., Cheung, L. Y. M., Daly, A. Z., Ajmal, A., Pérez Millán, M. I., Ozel, A. B., Kitzman, J. O., Mills, R. E., Li, J. Z., & Camper, S. A. (2016). Genetics of Combined Pituitary Hormone Deficiency: Roadmap into the Genome Era. *Endocrine Reviews*, *37*(6), Article 6. https://doi.org/10.1210/er.2016-1101

Glasgow, E., Karavanov, A. A., & Dawid, I. B. (1997). Neuronal and Neuroendocrine Expression oflim3,a LIM Class Homeobox Gene, Is Altered in Mutant Zebrafish with Axial Signaling Defects. *Developmental Biology*, *192*(2), 405–419. https://doi.org/10.1006/dbio.1997.8761

Gregory, L. C., & Dattani, M. T. (2020). The Molecular Basis of Congenital Hypopituitarism and Related Disorders. *The Journal of Clinical Endocrinology and Metabolism*, *105*(6), Article 6. https://doi.org/10.1210/clinem/dgz184

Gross-Thebing, T. (2020). RNAscope™ Multiplex Detection in Zebrafish. In B. S. Nielsen & J. Jones (Eds.), *In Situ Hybridization Protocols* (pp. 195–202). Springer US. https://doi.org/10.1007/978-1-0716-0623-0_12

Guner, B., Ozacar, A. T., Thomas, J. E., & Karlstrom, R. O. (2008). Graded hedgehog and establish the pars distalis and pars intermedia of the zebrafish adenohypophysis. *Endocrinology*, *149*(9), Article 9. https://doi.org/10.1210/en.2008-0315

Herzog, W., Zeng, X., Lele, Z., Sonntag, C., Ting, J.-W., Chang, C.-Y., & Hammerschmidt, M. (2003). Adenohypophysis formation in the zebrafish and its dependence on sonic hedgehog. *Developmental Biology*, *254*(1), Article 1. https://doi.org/10.1016/s0012-1606(02)00124-0

Hietamaki, J., Kärkinen, J., Iivonen, A.-P., Vaaralahti, K., Tarkkanen, A., Almusa, H., Huopio, H., Hero, M., Miettinen, P., & Raivio, T. (2022). Presentation and diagnosis of childhood-onset combined pituitary hormone deficiency: A single center experience from over 30 years. *eClinicalMedicine*, *51*, 101556. https://doi.org/10.1016/j.eclinm.2022.101556

Hypothalamus: What It Is, Function, Conditions & Disorders. (2023, May 11). Cleveland Clinic. https://my.clevelandclinic.org/health/articles/22566-hypothalamus

Karakaidos, P., Karagiannis, D., & Rampias, T. (2020). Resolving DNA Damage: Epigenetic Regulation of DNA Repair. *Molecules*, *25*(11), 2496. https://doi.org/10.3390/molecules25112496

Kaufmann, A., Mickoleit, M., Weber, M., & Huisken, J. (2012). Multilayer mounting enables long-term imaging of zebrafish development in a light sheet microscope. *Development*, *139*(17), Article 17. https://doi.org/10.1242/dev.082586

Knoepfler, P. (2022, March 1). *What is Matrigel, why a shortage, & alternatives?* The Niche. https://ipscell.com/2022/03/what-is-matrigel-why-a-shortage-alternatives/

Koontz, A., Urrutia, H. A., & Bronner, M. E. (2023). Making a head: Neural crest and ectodermal placodes in cranial sensory development. *Seminars in Cell & Developmental Biology*, *138*, 15–27. https://doi.org/10.1016/j.semcdb.2022.06.009

Lee, S., Sears, M. J., Zhang, Z., Li, H., Salhab, I., Krebs, P., Xing, Y., Nah, H.-D., Williams, T., & Carstens, R. P. (2020). Cleft lip and cleft palate in Esrp1 knockout mice is associated with alterations in epithelial-mesenchymal crosstalk. *Development (Cambridge, England)*, *147*(21), Article 21. https://doi.org/10.1242/dev.187369

Leslie, E. J., & Marazita, M. L. (2013). Genetics of Cleft Lip and Cleft Palate. *American Journal of Medical Genetics. Part C, Seminars in Medical Genetics*, *163*(4), Article 4. https://doi.org/10.1002/ajmg.c.31381

Lin, S.-Z., Ma, Q.-J., Pang, Q.-M., Chen, Q.-D., Wang, W.-Q., Li, J.-Y., & Zhang, S.-L. (2022). Novel compound heterozygous variants in the LHX3 gene caused combined pituitary hormone deficiency: A case report. *World Journal of Clinical Cases*, *10*(31), 11486–11492. https://doi.org/10.12998/wjcc.v10.i31.11486

Liu, N.-A., Ren, M., Song, J., Ríos, Y., Wawrowsky, K., Ben-Shlomo, A., Lin, S., & Melmed, S. (2008). In vivo time-lapse imaging delineates the zebrafish pituitary proopiomelanocortin lineage boundary regulated by FGF3 signal. *Developmental Biology*, *319*(2), Article 2. https://doi.org/10.1016/j.ydbio.2008.03.039

Netchine, I., Sobrier, M.-L., Krude, H., Schnabel, D., Maghnie, M., Marcos, E., Duriez, B., Cacheux, V., Moers, A. v, Goossens, M., Grüters, A., & Amselem, S. (2000). Mutations in LHX3 result in a new syndrome revealed by combined pituitary

hormone deficiency. *Nature Genetics*, *25*(2), Article 2. https://doi.org/10.1038/76041

Nica, G., Herzog, W., Sonntag, C., & Hammerschmidt, M. (2004). Zebrafish pit1 mutants lack three pituitary cell types and develop severe dwarfism. *Molecular Endocrinology (Baltimore, Md.)*, *18*(5), 1196–1209. https://doi.org/10.1210/me.2003-0377

Nica, G., Herzog, W., Sonntag, C., Nowak, M., Schwarz, H., Zapata, A. G., & Hammerschmidt, M. (2006). Eya1 is required for lineage-specific differentiation, but not for cell survival in the zebrafish adenohypophysis. *Developmental Biology*, *292*(1), Article 1. https://doi.org/10.1016/j.ydbio.2005.12.036

Pituitary Gland: What It Is, Function & Anatomy. (2022, November 26). Cleveland Clinic. https://my.clevelandclinic.org/health/body/21459-pituitary-gland

pomca (all cells): Daniocell. (n.d.). Retrieved January 26, 2024, from https://daniocell.nichd.nih.gov/gene/P/pomca/pomca.html

Prakash, K., Diederich, B., Heintzmann, R., & Schermelleh, L. (2022). Super-resolution microscopy: A brief history and new avenues. *Philosophical Transactions of the Royal Society A: Mathematical, Physical and Engineering Sciences*, *380*(2220), Article 2220. https://doi.org/10.1098/rsta.2021.0110

Riedl, J., Crevenna, A. H., Kessenbrock, K., Yu, J. H., Neukirchen, D., Bista, M., Bradke, F., Jenne, D., Holak, T. A., Werb, Z., Sixt, M., & Wedlich-Soldner, R. (2008). Lifeact: A versatile marker to visualize F-actin. *Nature Methods*, *5*(7), 605–607. https://doi.org/10.1038/nmeth.1220

RNAscope Multiplex Fluorescent V2 Assay | In Situ Hybridization, RNA-ISH | ACDBio. (n.d.). Retrieved January 29, 2024, from https://acdbio.com/rnascope-multiplex-fluorescent-v2-assay

Saha, K., & Jaenisch, R. (2009). Technical challenges in using human induced pluripotent stem cells to model disease. *Cell Stem Cell*, *5*(6), Article 6. https://doi.org/10.1016/j.stem.2009.11.009

Schlosser, G. (2006). Induction and specification of cranial placodes. *Developmental Biology*, *294*(2), 303–351. https://doi.org/10.1016/j.ydbio.2006.03.009

Sheng, H. Z., Moriyama, K., Yamashita, T., Li, H., Potter, S. S., Mahon, K. A., & Westphal, H. (1997). Multistep Control of Pituitary Organogenesis. *Science*, *278*(5344), 1809–1812. https://doi.org/10.1126/science.278.5344.1809

Sheng, H. Z., Zhadanov, A. B., Mosinger, B., Fujii, T., Bertuzzi, S., Grinberg, A., Lee, E. J., Huang, S. P., Mahon, K. A., & Westphal, H. (1996). Specification of pituitary cell lineages by the LIM homeobox gene Lhx3. *Science (New York, N.Y.)*, *272*(5264), 1004–1007. https://doi.org/10.1126/science.272.5264.1004

Singh, S., & Groves, A. K. (2016). The Molecular Basis of Craniofacial Placode Development. *Wiley Interdisciplinary Reviews. Developmental Biology*, *5*(3), Article 3. https://doi.org/10.1002/wdev.226

Suga, H. (2016). Recapitulating Hypothalamus and Pituitary Development Using Embryonic Stem/Induced Pluripotent Stem Cells. In D. Pfaff & Y. Christen (Eds.), *Stem Cells in Neuroendocrinology*. Springer. http://www.ncbi.nlm.nih.gov/books/NBK435791/

Teame, T., Zhang, Z., Ran, C., Zhang, H., Yang, Y., Ding, Q., Xie, M., Gao, C., Ye, Y., Duan, M., & Zhou, Z. (2019). The use of zebrafish (Danio rerio) as biomedical models. *Animal Frontiers*, *9*(3), Article 3. https://doi.org/10.1093/af/vfz020

Toda, C., Santoro, A., Kim, J. D., & Diano, S. (2017). POMC Neurons: From Birth to Death. *Annual Review of Physiology*, *79*(1), 209–236. https://doi.org/10.1146/annurev-physiol-022516-034110

Ueharu, H., Yoshida, S., Kikkawa, T., Kanno, N., Higuchi, M., Kato, T., Osumi, N., & Kato, Y. (2017). Gene tracing analysis reveals the contribution of neural crest-derived cells in pituitary development. *Journal of Anatomy*, *230*(3), Article 3. https://doi.org/10.1111/joa.12572

Vishnopolska, S. A., Mercogliano, M. F., Camilletti, M. A., Mortensen, A. H., Braslavsky, D., Keselman, A., Bergadá, I., Olivieri, F., Miranda, L., Marino, R., Ramírez, P., Pérez Garrido, N., Patiño Mejia, H., Ciaccio, M., Di Palma, M. I., Belgorosky, A., Martí, M. A., Kitzman, J. O., Camper, S. A., & Pérez-Millán, M. I. (2021). Comprehensive Identification of Pathogenic Gene Variants in Patients With Neuroendocrine Disorders. *The Journal of Clinical Endocrinology and Metabolism*, *106*(7), Article 7. https://doi.org/10.1210/clinem/dgab177

Walker, R. M., Brewer, G. A., Lee, M. J., Petrovsky, N., & van Witteloostuijn, A. (2019). Best Practice Recommendations for Replicating Experiments in Public Administration. *Journal of Public Administration Research and Theory*, *29*(4), Article 4. https://doi.org/10.1093/jopart/muy047

Warzecha, C. C., Jiang, P., Amirikian, K., Dittmar, K. A., Lu, H., Shen, S., Guo, W., Xing, Y., & Carstens, R. P. (2010). An ESRP-regulated splicing programme is abrogated during the epithelial–mesenchymal transition. *The EMBO Journal*, *29*(19), Article 19. https://doi.org/10.1038/emboj.2010.195

Yang, Y., & Carstens, R. P. (2017). Alternative splicing regulates distinct subcellular localization of Epithelial splicing regulatory protein 1 (Esrp1) isoforms. *Scientific Reports*, *7*(1), 3848. https://doi.org/10.1038/s41598-017-03180-3

Zhu, X., Lin, C. R., Prefontaine, G. G., Tollkuhn, J., & Rosenfeld, M. G. (2005). Genetic control of pituitary development and hypopituitarism. *Current Opinion in Genetics & Development*, *15*(3), 332–340. https://doi.org/10.1016/j.gde.2005.04.011

Zimmer, B., Piao, J., Ramnarine, K., Tomishima, M. J., Tabar, V., & Studer, L. (2016). Derivation of Diverse Hormone-Releasing Pituitary Cells from Human Pluripotent Stem Cells. *Stem Cell Reports*, *6*(6), Article 6. https://doi.org/10.1016/j.stemcr.2016.05.005